arXiv:astro-ph/0408117v3 21 Jul 2005

New Reference Galaxy Standards for H I Emission Observations

K. O'Neil[1]
NRAO; PO Box 2; Green Bank, WV 24944
koneil@nrao.edu

ABSTRACT

We have taken advantage of the improved baselines and higher sensitivity available with the upgraded Arecibo 305m telescope to create a new H I spectral line catalog of disk galaxies which can be used as a reference catalog for anyone interested in 21-cm spectral line work. In all 108 galaxies were observed, covering 24h of the sky at declinations between $0^\circ < \delta < 36^\circ$ and velocities between 0 – 25,000 km s^{-1}. The majority of the galaxies were observed at least two times on different nights to avoid problems with radio frequency intereference, baselines fluctuations, etc. Comparing our measured values with all those available in the literature show that while large individual variations may exist, the average differences between the measurements to be zero. In all we have considerable confidence in our measurements, and the resultant catalog should be extremely useful as a well defined reference catalog for anyone interested in 21-cm spectral line work.

Subject headings: galaxies: distances and redshifts – galaxies:masses – galaxies:spiral – galaxies: gas – radio lines: galaxies

1. Introduction

The 21-cm neutral hydrogen line is possibly the most commonly observed spectral line by centimeter wavelength telescopes. Yet a brief perusal through any collection of of H I observations on a gas-rich galaxy will often find flux measurements varying by 5% – 100%, or more (Huchtmeier & Richter 1989; NED[1]). The reasons behind these discrepancies are many-fold. The simplest explanation for the differences is various telescopes' beam sizes and shapes. That is, observing a galaxy with H I spread over a $10'$ region with the Arecibo 305m telescope ($3.6'$ FWHM beam at 1.4 GHz) would certainly result in a different flux measurement than if that same object were observed with the Green Bank Telescope ($9.2'$ FWHM beam at 1.4 GHz). Yet while the differences in beam sizes and patterns may account for some of the discrepancies seen, it cannot be the only explanation, as only a fraction of the known galaxies have diameters larger than the Arecibo beam. (Roughly 15% of the galaxies in the UGC catalog have optical diameters $>2'$ – Nilson 1973.) Instead, or in addition, to the previous explanation, the discrepancies in the different measurements may be due to inaccuracies in the hardware and software used for data taking and analysis. These can include pointing offsets, unstable hardware resulting in baseline variations, rapid (compared to the frequency of measurements) temperature fluctuations, poor telescope focus, and over- or under-estimates of line flux due to inaccurate baseline fitting. In addition, line flux measurements can suffer from erroneous values of both the astronomical (gain) and system (temperature) calibration values due to either inaccuracies in the measurements or or measurement which are sampled too sparsely in time, frequency, or position to accurately reflect the system.

As a result of the variations found in the different H I galaxy catalogs, astronomers wishing to obtain accurate flux values for a given galaxy are often forced to average the various measurements found in published catalogs, invoke a selection effect on the previous measurements, assuming some measurements are more accurate than others, or simply re-observe the objects of interest with the hope that their data will be be more reliable, on average, than that found in the literature. While all of the above methods are sound and should be encouraged, they can also be impractical, particularly when the researcher is interested in comparing their own results against a consistent, well-defined catalog with readily understood errors. This is not meant to imply that catalogs of H I measurements found in

[1]Work done while at Arecibo Observatory

[1]NED, the NASA/IPAC Extragalactic Database, is operated by the Jet Propulsion Laboratory, California Institute of Technology, under contract with the National Aeronautics and Space Administration.

the literature are in general unreliable, simply that as the purpose of the majority of catalogs is to look for statistical information regarding the neutral hydrogen content in the studied galaxies, the errors associated with the measurements for an individual galaxy can be fairly high.

Previous efforts have been made to generate extremely accurate lists of H I in galaxies for calibration and references purposes (e.g. Tifft 1992; Schneider, et al. 1992; Huchtmeier & Richter 1988; Baiesi-Pillastrini & Palumbo 1986). However, as a result of its recent upgrade (Salter 2002), the Arecibo 305m telescope now offers unprecedented stable baselines, increased sensitivity, and extremely good pointing. As a consequence, we have taken advantage of Arecibo's exceptional performance and have observed over 100 galaxies with the aim of offering a catalog of H I observations which can be used as a reference catalog for anyone interested in 21-cm spectral line work. All of the data and results for this project are publicly available online at both http://www.gb.nrao.edu/∼koneil/HIsurvey and http://www.naic.edu/∼astro/HIsurvey.

2. Catalog Selection

The galaxies chosen cover the complete Arecibo sky ($-1^\circ < \delta < 38.5^\circ$), with at least three galaxies within any given hour of LST. Additionally, an attempt was made to cover velocity space from 0 – 25,000 km s^{-1}. However, our requirement that the objects' signal-to-noise be reasonably high within a few minutes of observation (detailed below) resulted in the majority of the objects lying at <8,000 km s^{-1}. To remedy this problem, a few objects were observed which do not meet the signal-to-noise criteria. These objects are noted in Table 1, which also gives a complete listing of galaxies observed and their coordinates, and Figures 1 and 2 show the distribution of the galaxies in velocity, Declination, and Right Ascension space.

In addition to the above constraints, the selection for the catalog was based on five major criteria. The observed galaxies should:

- Have previous 21-cm line measurements indicating an emission of at least 10 mJy. This ensures a signal-to-noise ratio at Arecibo of >8 after five minutes of on-source observation (using 8.5 km s^{-1} channel^{-1} resolution);
- Have an optical diameter, $D_{25} \leq 2'$ to avoid the galaxy's H I from extending past the ∼3.5′ Arecibo beam;
- Be isolated to a 10′, 1000 km s^{-1} radius to avoid

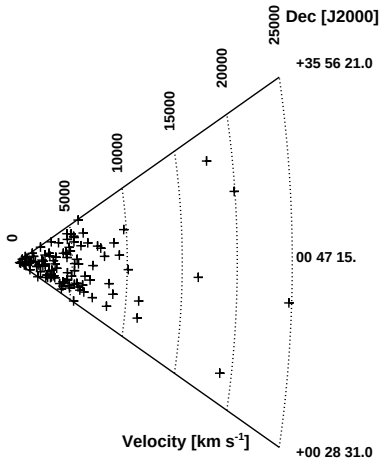

Fig. 1.— Distribution of observed galaxies in Dec.-velocity space

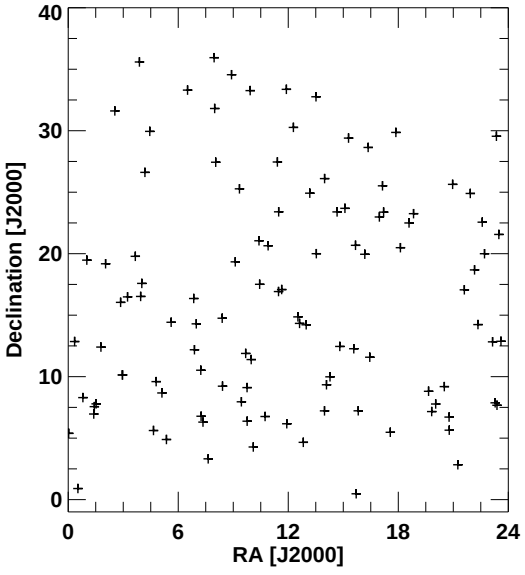

Fig. 2.— Distribution of observed galaxies in RA-Dec space.

contamination through the beam side-lobes;

- Have no significant continuum emission. This avoids residual standing waves which arise from Arecibo's partially blocked aperture (Ghosh & Salter 2001).

No information regarding the distribution of the H I for the observed galaxies was used in determining the catalog, in large part due to the fact that such information is not available for many of the galaxies observed. As a result, any discontinuities or asymmetries in the galaxies' H I distribution was not accounted by this project.

3. Observations, Calibration, and Data Reduction

Data was taken with the L-narrow receiver between Aug, 2001 - July, 2002. Each galaxy was observed with two polarization channels at two different resolutions (12.5 MHz/2048 channels for 1.3 km s^{-1} channel^{-1} resolution and 6.25 MHz/2048 channels for 0.63 km s^{-1} channel^{-1} resolution at 1420 MHz). Standard position switching techniques were used for all observations, tracking the same azimuth and zenith angle for the off-source observation as for the on-source observation to reduce differences in the baseline shapes. Observations were typically 5 minutes on-source and 5-minutes off-source, although the total time was occasionally reduced if the telescope scheduling required it. Temperature measurements (with a calibrated noise diode) were made after each on+off observation pair. Details on the noise diode calibration can be found on the Arecibo web pages at http://www.naic.edu/∼astro/Lnarrow.

A gain curve for the telescope was obtained through reducing all observations taken of standard continuum calibrators, by any project, during the observing period. A complete description of the procedures used to determine the gain curve in this manner can be found in Heiles (2001). Additionally, observations were made of standard continuum calibrators every 2-3 hours during the project observations, with the results checked against the determined telescope gain, to insure no anomalous behavior occurred in the hardware during observations.

The variation between any individual measurement of a calibration source and the gain measurement could range as high as 20%, particularly in Arecibo's outer declination reaches ($32^\circ \leq \delta \leq 36^\circ$). Smoothing the individual measurements onto a two-dimensional fit reduces the overall calibration error to less then 10%. To further reduce the error, sources were observed at angles between 2° – 14° from the zenith whenever possible to avoid the regions where the residuals of the gain curve fit were high. Finally, each object was observed a number of different times, at different LSTs, so that any variations in the determined two-dimensional gain curve are minimized. The the end result is flux measurements which should be reliable at the 5% level, or better.

To reduce the data, first the individual scans for each observation were averaged, and the on- and off-source observations were combined. The correct value for the gain curve was obtained using the average azimuth and zenith from the individual one second data dumps. The gain and system temperature corrections were made after combining the on- and off-source observations. At this point baselines were subtracted (using first order polynomials) and the flux, heliocentric velocity, and velocity widths were determined from each individual observation. This allowed for the determination of the potential ranges of values which an astronomer might see when observing a given object. Finally, the individual observations (without baseline subtractions) were combined to give the highest possible signal-to-noise for a given galaxy. Baselines were subtracted and the flux, heliocentric velocity, and velocity widths were determined from this averaged observation. In each case baseline fitting was done using a minimum of 200 frequency channels on each side of the line of interest. In sum, the observed, reduced data was

$$\mathrm{Spectra} \;=\; \frac{\langle \mathrm{On_i} \rangle \;-\; \langle \mathrm{Off_i} \rangle}{\langle \mathrm{Off_i} \rangle} \;\times\; \frac{\mathrm{T_{sys}}}{\mathrm{Gain}}$$

$$\mathrm{Final\ Spectra} \;=\; \langle \mathrm{Spectra_i} \rangle$$

All baselines appeared to be best fit (in the χ^2 sense) by first order polynomials. Any discrepancies between the baseline fits and the data are reflected in the r.m.s. measurements obtained.

4. Final Results and Error Calculations

The final results and associated errors are reported in Table 1, and the 8.5 km s^{-1} resolution spectra are in Figure 3. (The 1.3 and 0.65 km s^{-1} resolution spectra are online at http://www.gb.nrao.edu/∼koneil/HIsurvey.) Each spectra was analyzed three times, at three different resolutions – 0.65 km s^{-1}, 1.3 km s^{-1}, and 8.5 km s^{-1}, with the 8.5 km s^{-1} resolution data obtained through boxcar averaging the 0.65 km s^{-1} resolution data. The baseline fit region (described in the last section) was also used for determining the r.m.s. of the spectra. The flux was found by fitting (by eye) the outer edges of the galaxy, and all flux within the de-

fined regions was summed. The velocity widths were determined at 20% and 50% of the mean value of the

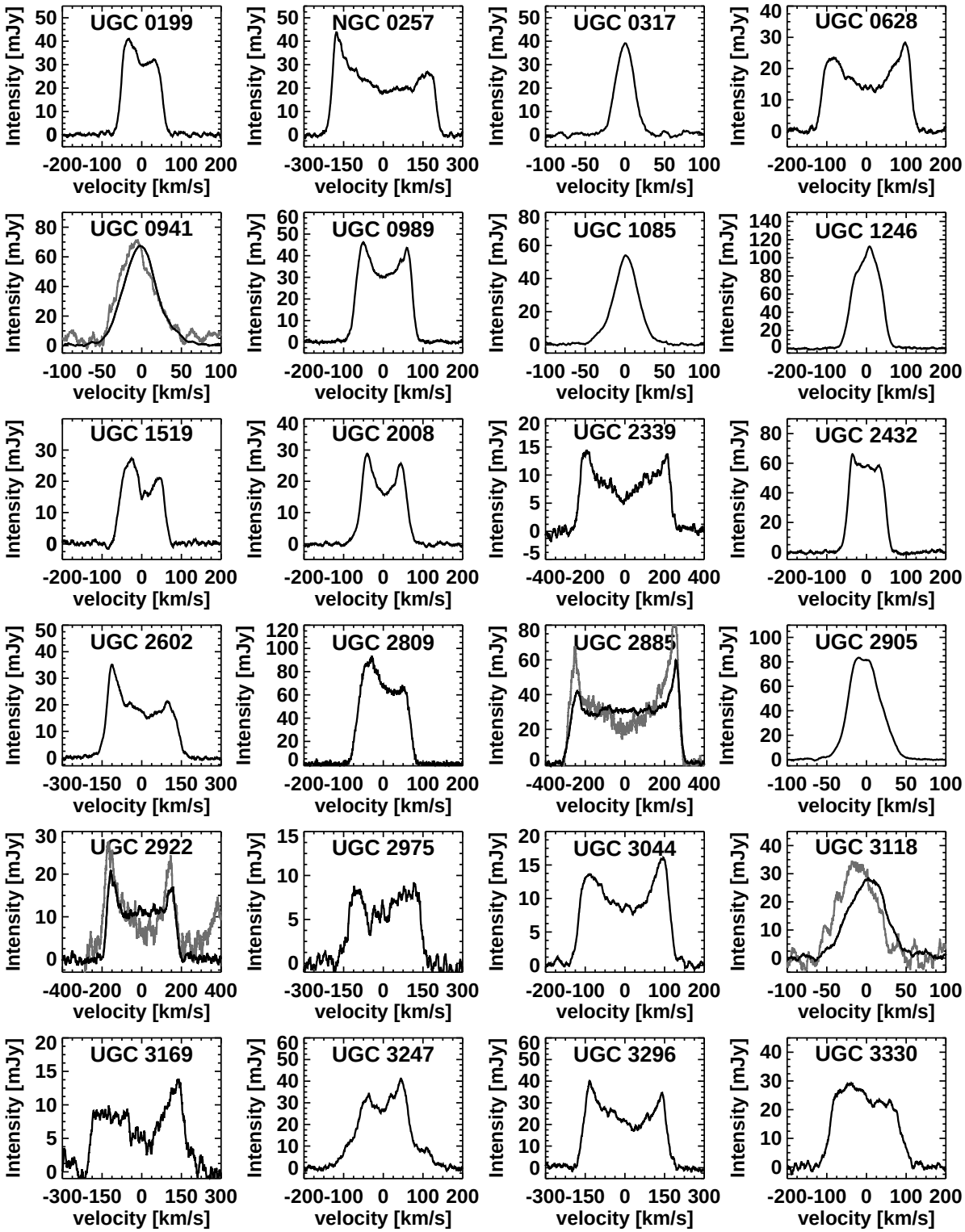

Fig. 3.— 8.5 km s^{-1} resolution spectra of the observed galaxies. The black lines are the Arecibo data and the gray lines are the GBT data.

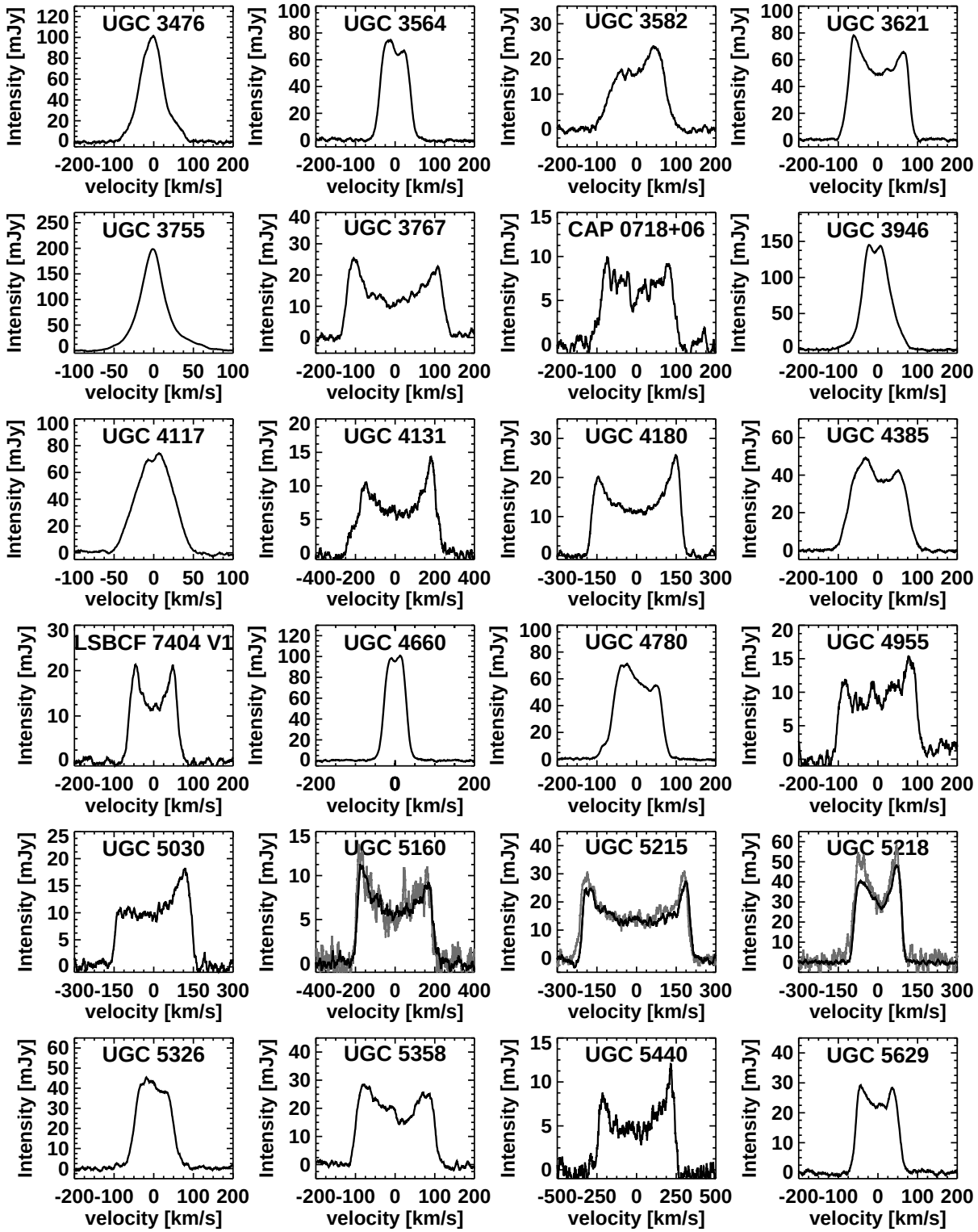
UGC 3476
UGC 3564
UGC 3582
UGC 3621
UGC 3755
UGC 3767
CAP 0718+06
UGC 3946
UGC 4117
UGC 4131
UGC 4180
UGC 4385
LSBCF 7404 V1
UGC 4660
UGC 4780
UGC 4955
UGC 5030
UGC 5160
UGC 5215
UGC 5218
UGC 5326
UGC 5358
UGC 5440
UGC 5629
Intensity [mJy]
velocity [km/s]

Fig. 3.— *cont.*

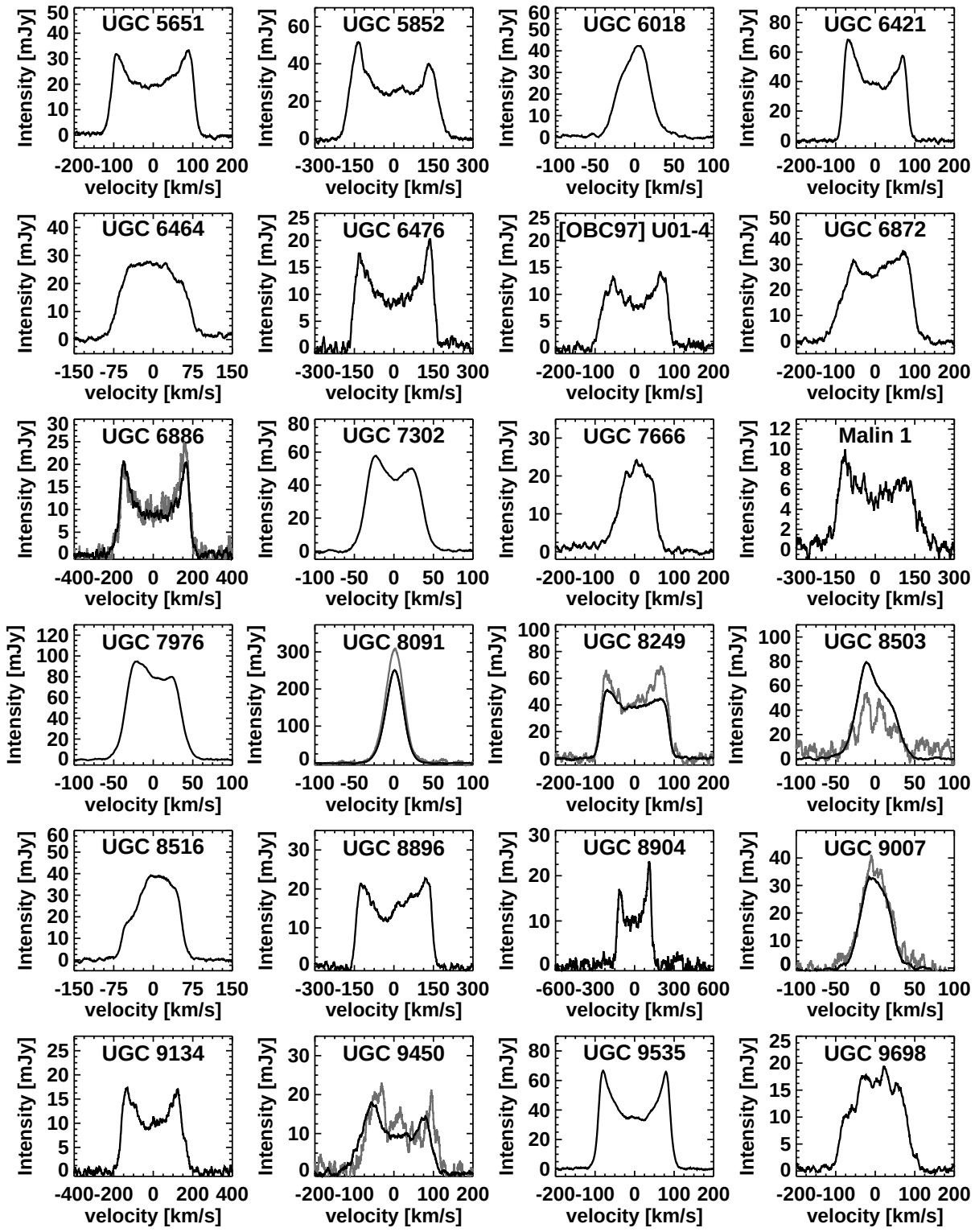
UGC 5651
UGC 5852
UGC 6018
UGC 6421
UGC 6464
UGC 6476
[OBC97] U01-4
UGC 6872
UGC 6886
UGC 7302
UGC 7666
Malin 1
UGC 7976
UGC 8091
UGC 8249
UGC 8503
UGC 8516
UGC 8896
UGC 8904
UGC 9007
UGC 9134
UGC 9450
UGC 9535
UGC 9698
Intensity [mJy]
velocity [km/s]

Fig. 3.— *cont.*

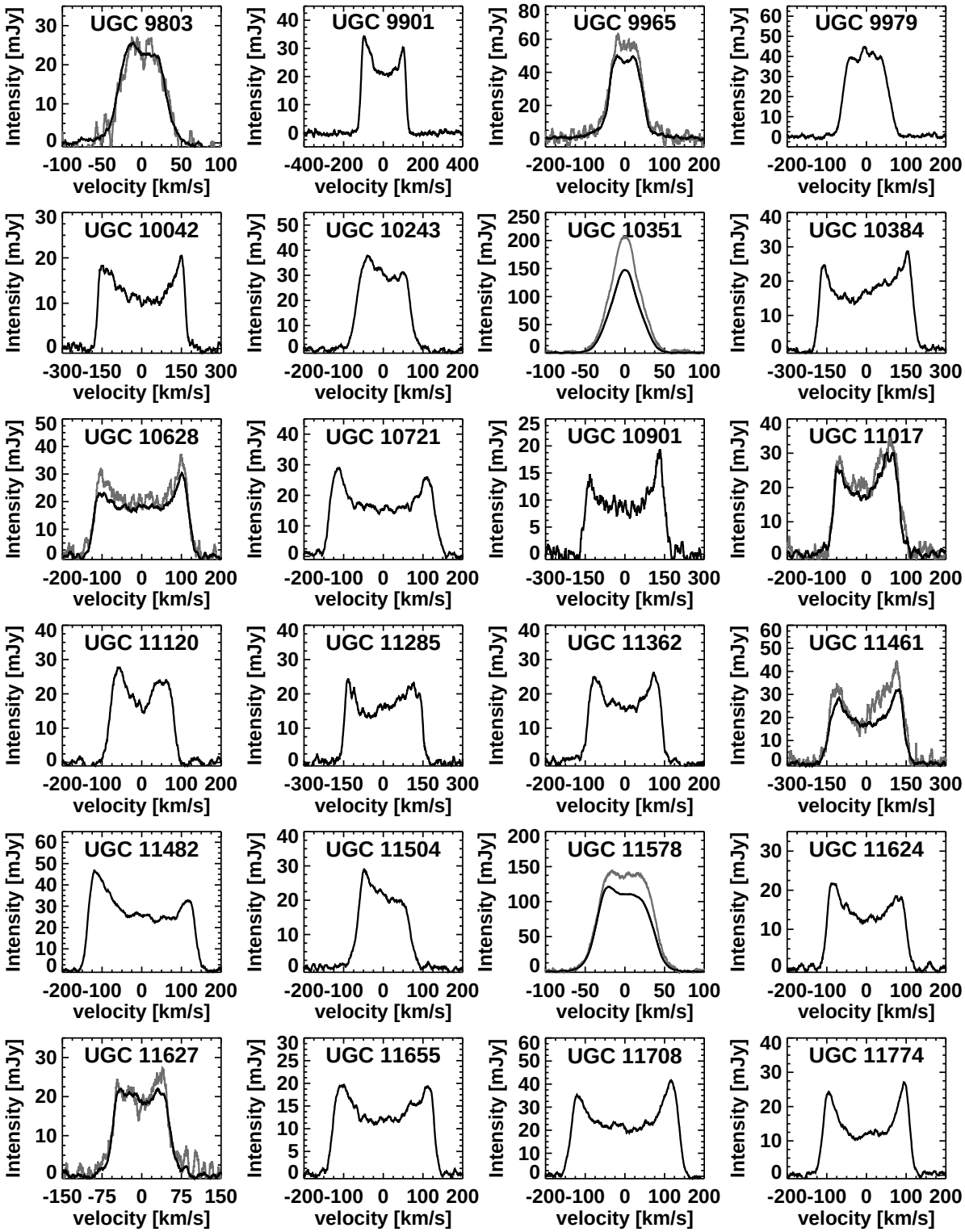
UGC 9803
UGC 9901
UGC 9965
UGC 9979
UGC 10042
UGC 10243
UGC 10351
UGC 10384
UGC 10628
UGC 10721
UGC 10901
UGC 11017
UGC 11120
UGC 11285
UGC 11362
UGC 11461
UGC 11482
UGC 11504
UGC 11578
UGC 11624
UGC 11627
UGC 11655
UGC 11708
UGC 11774
Intensity [mJy]
velocity [km/s]

Fig. 3.— *cont.*

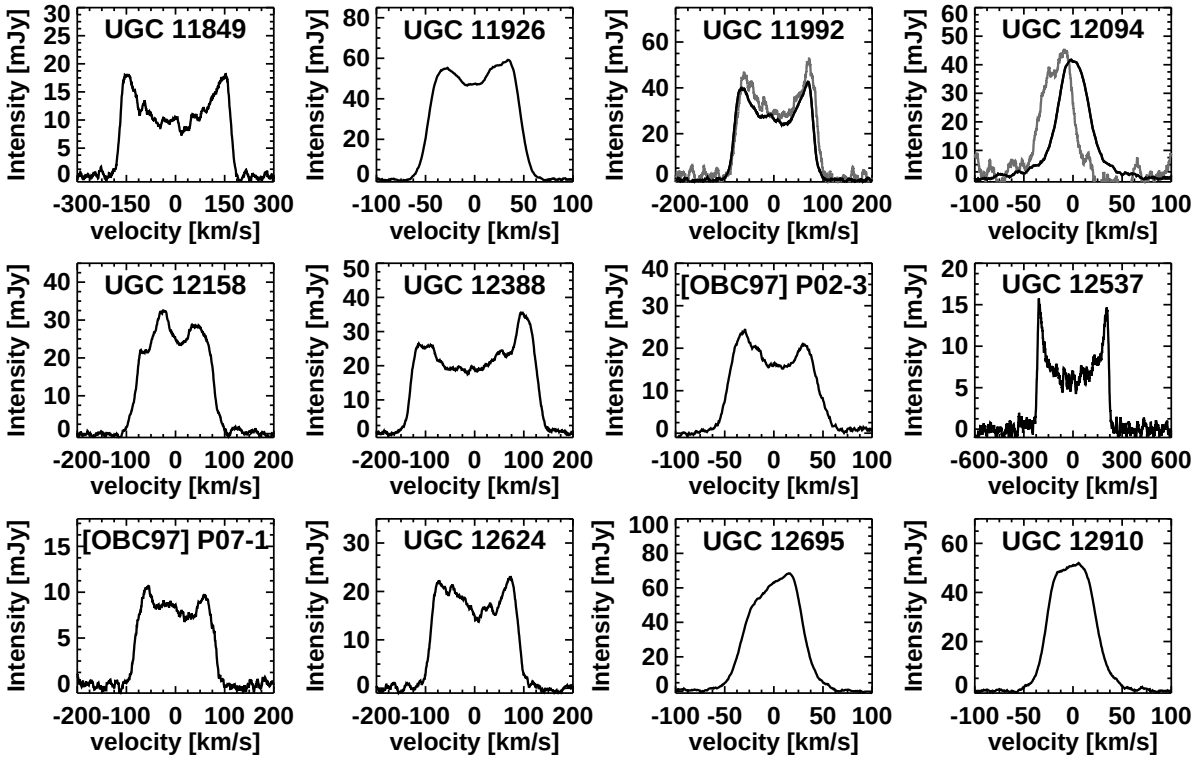
UGC 11849
UGC 11926
UGC 11992
UGC 12094
UGC 12158
UGC 12388
[OBC97] P02-3
UGC 12537
[OBC97] P07-1
UGC 12624
UGC 12695
UGC 12910
Intensity [mJy]
velocity [km/s]

Fig. 3.— *cont.*

selected region. Finally, the heliocentric velocity is equal to $1/2 \times (v_{high} - v_{low})$, where v_{low} and v_{high} are equal to the low and high values of the heliocentric velocity at 20% or 50% times mean value of two H I peaks.

The results from the data analysis were then combined, and errors determined, as described below. For each galaxy both the individual observations and the average of the individual observations were analyzed. The results from the averaged observations provide the most accurate measurements and are reported in Table 1. The individual measurements were used only to determine the range of values found, and are reported online at http://www.gb.nrao.edu/∼koneil/HIsurvey.

4.1. Heliocentric Velocity

The reported value for the heliocentric velocity comes from taking the mean value of the three heliocentric velocity measurements obtained from the averaged (high signal-to-noise) spectra. To determine the error for this value, first the r.m.s. error at each velocity resolution was determined through averaging the velocity measurements from the individual (not averaged) observations. The errors from the three velocity resolution were then added, in quadrature, to determine the final reported error.

4.2. Flux

Fluxes were determined at each velocity resolution from the averaged (high signal-to-noise) spectra of each galaxy. The r.m.s. of the averaged spectra was found through examining a minimum of 200 channels on either side of the spectral line of interest. The observational error was then determined as $\sigma_{flux,obs} = \sqrt{N} \times (channel\ width) \times \sigma_{rms}$, where N is the number of channels (the velocity width divided by the channel width), and σ_{rms} is the rms error calculated. The final error was determined through adding (in quadrature) the observational error and a 5% error assumed for the gain curve. (See Section 3 for a description of the gain curve error).

4.3. Velocity Widths

Velocity widths were found at both 20% and 50% of the peak flux for each velocity resolution using the averaged (high signal-to-noise) spectra of every galaxy. The error reported for the velocity widths are the r.m.s. errors from the average of the individual (not averaged) observations. On the occasion where the r.m.s. error was less than half the channel resolution, the error was set equal to half the channel resolution.

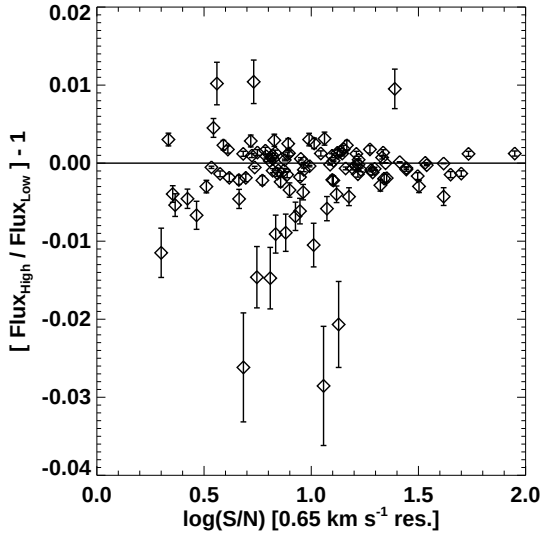

Fig. 4.— Comparison of the r.m.s. differences for the lowest and highest resolution data measured against the average signal-to-noise of the spectral line. While the average difference between the two resolutions ($\frac{Flux_{high}}{Flux_{low}} - 1$) is zero, a marked difference from zero for the r.m.s. can be seen for the lower S/N. (Average signal to noise was found through dividing the total flux by the r.m.s. noise for each galaxy.)

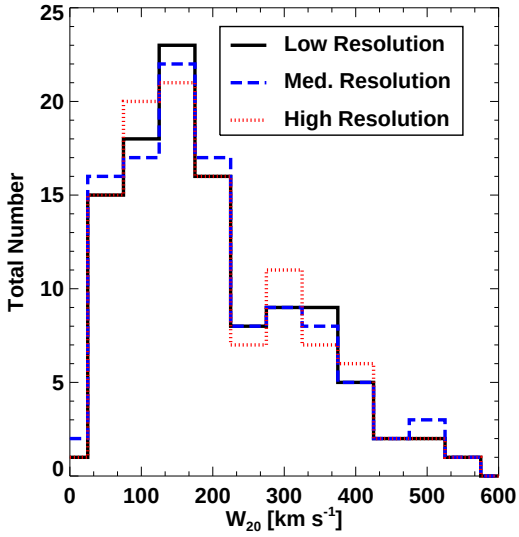

Fig. 5.— A histogram of the W_{20} distribution for the observed galaxies. The average signal -to-noise for the three different resolutions is shown. The solid line is the 8.5 km s^{-1} resolution, the dashed line is the 1.3 km s^{-1} resolution, and the dotted line is the 0.65 km s^{-1} resolution.

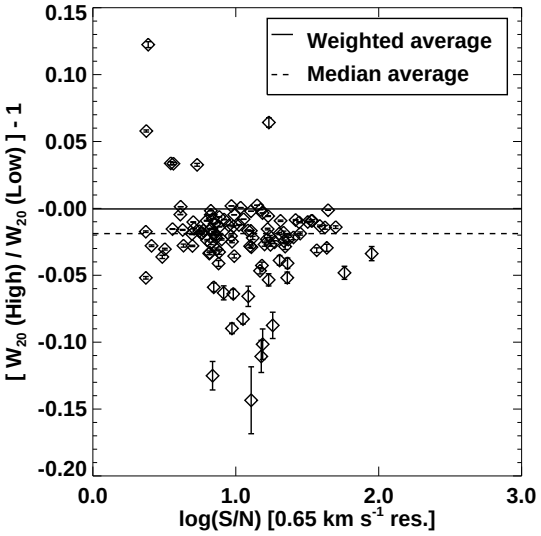

Fig. 6.— Comparison of the lowest and highest resolution data measured against the average signal-to-noise of the spectral line. (Average signal to noise was found through dividing the total flux by the velocity width of each galaxy.) The solid and dashed red lines simply mark the weighted (by $1/\sigma^2$) and unweighted averages of the differences. The weighted average lies at zero.

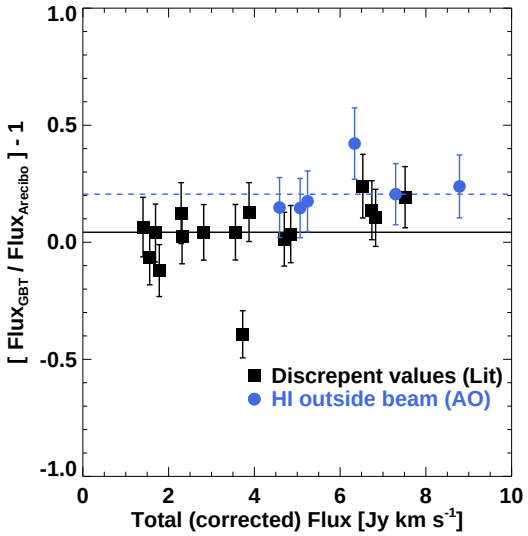

Fig. 7.— Comparison between the fluxes found with the Arecibo and Green Bank Telescopes. the same is broken into two groups – objects which we believe our Arecibo measurements to be correct (squares) and objects which we believe the flux extends well beyond the Arecibo beam (circles). The lines show the median values of the two groups. See Section 6 for more information on these sources.

5. Signal-to-Noise vs. High Resolution

One interesting observational effect which can be studied with our observations is the trade-off between high frequency (channel) resolution and high signal-to-noise (lower resolution). The average S/N is 14, 19, and 46 and the minimum (maximum) S/N seen are 2 (89), 3 (122), and 7 (310) for the 0.65, 1.3, and 8.5 km s^{-1} $channel^{-1}$ resolutions, respectively. The lowest S/N for all three resolutions are from the observations of CAP 0718+06 and the highest from UGC 8091. Figure 4 shows the ratio of the fluxes found in the high (0.65 km s^{-1}) and low (8.5 km s^{-1}) resolution plots.

We also compared the flux values obtained for the various channel resolutions, and found that other than at the very. low S/N end of the distribution, the overall flux distribution is extremely similar between the low and high resolution images. However, looking at the individual comparisons between the low and high resolution measurements it is (not surprisingly) clear that the higher the overall signal-to-noise the more consistent the flux measurements are, with the differences between the measurements being essentially zero once the S/N reaches $\sim$30.

Figures 5 and 6 show a comparison between the measured (W_{20}) velocity widths and the velocity resolution. The results match what one would naïvely believe – the higher resolution spectra provide the most accurate measurements of the velocity widths. That is, one can see that the higher resolution images have, on average, slightly narrower velocity widths than the lower resolution spectra.

5.1. Green Bank Telescope Observations

After the Arecibo observations were analyzed, the fluxes of a number of objects were found to differ significantly from the literature values of the same sources. To check the Arecibo results, we re-observed the most discrepant sources (as described in Section 6) using the Robert C. Byrd Green Bank Telescope (GBT). All GBT observations took place between 19 April – 14 May, 2004. Each galaxy was observed in two separate (linear) polarizations with a 12.5 MHz bandwidth and 32767 channels/polarization (0.08 km s^{-1} resolution). The data was then boxcar smoothed to 8 km s^{-1} resolution, to approximate the resolution of the Arecibo observations. Standard position switching techniques were used for all observations, tracking the same azimuth and zenith angle for the off-source and on-source observations to reduce any differences in baseline shapes. The on- and off-source observations were 5 minutes each with a 10 second on+off observation of a bright, calibrated, noise diode (the 'high-cal')

to determine the system temperature.

The telescope gain was determined through observing 3-4 standard continuum calibrators each night. As the gain of the GBT at 1.4 GHz does not change significantly until one observes a source at low zenith angle (Ghiho, et.al 2001), no sources were observed at zenith angles less than 45°. As a result, the gain found with the continuum calibrators was applied to all sources without regard to their sky position. The variation between the calibration source measurements was between 5–10%. The calibration of the sources should not be trusted to better than this level.

Data reduction took place using the same methods (and routines) as for the Arecibo data, with the exception that second order baselines were fit to the data when necessary.

The measurements from the GBT observations are given in Table 2, the spectra are shown in Figure 3. A comparison between the GBT and Arecibo measurements is shown in Figure 7. The average offset between the GBT and Arecibo measurements of sources which do not have H I extended outside the 3.5′ Arecibo beam (the black symbols in Figure 7) is 4±20%, essentially zero.

6. Comparison with Literature and GBT Values

Figure 8 shows a comparison between the velocity width (W_{20}) in our survey versus all values found in the literature (searched through NED – the NASA Extragalactic Database, and listed in Table 3). Similar plots are shown in Figures 9 and 10 for the flux measurements, using the final (gain, beam, and pointing-corrected) values in the literature for the comparison. In all plots the literature values are split into two categories – measurements previously made at Arecibo, and measurements made at any other telescope. Errors for the literature value typically came directly from the published value. In the cases where no value was published, the flux error was estimated from multiplying the reported velocity width by the reported r.m.s. error. When no error was reported for the measured velocity widths, the error was estimated to be equal to half a velocity channel. Errors used are given in Table 3, and a description of the comparisons is below.

6.1. Velocity Width Comparisons

For the velocity width measurement comparisons (Figure 8), the weighted average and mean of the differences between our observations and those found in the literature are zero regardless of the telescope used for the observations. This shows there are no systematic errors affecting our results. In fact, there are only

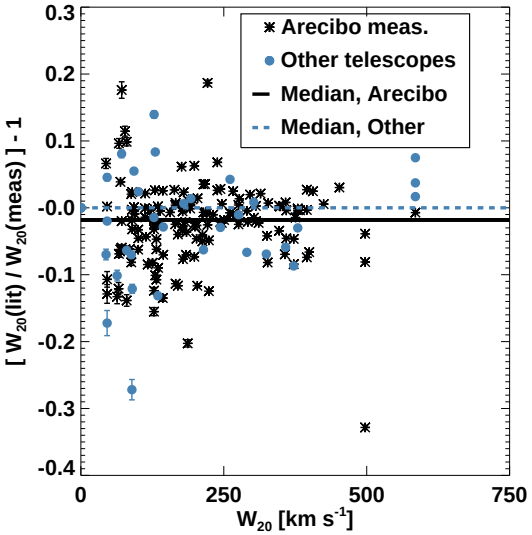

Fig. 8.— Comparison between the velocity widths of our survey with the values found in the literature. To insure accuracy in the comparisons, the data from our survey was smoothed to the same resolution as that commonly found in previous observations (8.5 km s^{-1} at 1420 MHz). Additionally, the literature sample was broken into two categories - previous Arecibo Observations (all done before the upgrade) and those observations taken at other radio telescopes. No significant different from zero is seen for the mean of the difference between out measurements and those in the literature. The comparison between the value of UGC 9007 found by our survey and that found in (Bothun et al. 1985a) is not shown on the plot. It should lie at W_{20}=76 km s^{-1}, difference=1.35.

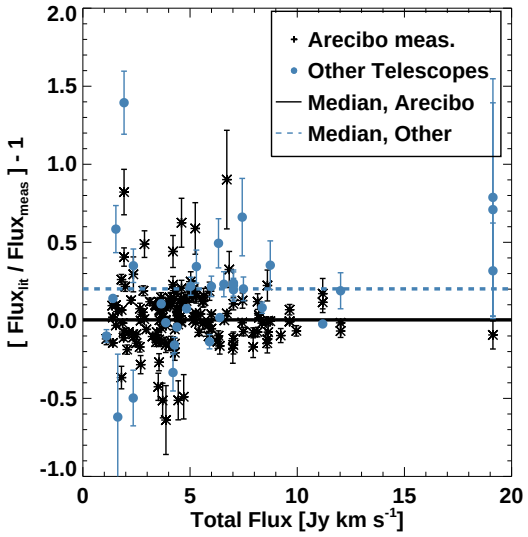

Fig. 9.— A comparison between the fluxes found with our survey and the values found in the literature. To insure accuracy in the comparison, the data from our survey was smoothed to the same resolution as that commonly found in previous observations (8.5 km s^{-1} at 1420 MHz). Additionally, the literature sample was broken into two categories - previous Arecibo Observations (all done before the upgrade) and those observations taken at other radio telescopes. This plot shows a a direct comparison between our data and that in the literature. The mean of the unweighted flux differences lie at 0.00 and 0.19 for the Arecibo and non-Arecibo samples, respectively.

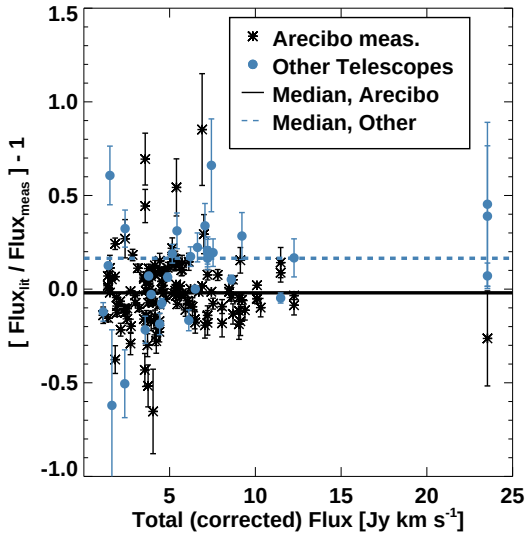

Fig. 10.— Comparison between the fluxes found with our survey and the values found in the literature. To insure accuracy in the comparisons, the data from our survey was smoothed to the same resolution as that commonly found in previous observations (8.5 km s^{-1} at 1420 MHz). Additionally, the literature sample was broken into two categories - previous Arecibo Observations (all done before the upgrade) and those observations taken at other radio telescopes. This plot compares our data after it has been corrected for the beam width (see Section 6). The unweighted medians lie at -0.02 and 0.14 for the Arecibo and non-Arecibo samples, respectively.

3 observations (out of a total of 186) which vary by more than 20% from the value our measured values. In each case follow-up observations taken with the GBT confirmed our Arecibo measurements. The 'errant' literature values are:

- **UGC 3118:** There are two measurements of this galaxy in the literature, one of which agrees with our Arecibo and GBT measurements to within the errors, and one which does not. The 'errant' measurement was made by Schneider, Thuan, Mangum, & Miller (1992) with the Green Bank 300′ telescope. Schneider, et.al list their observation as potentially confused with another source, which likely explains the difference in measurements.

- **UGC 9007:** Three values for the H I properties of UGC 9007 can be found in the literature, two which match that found by our Arecibo and GBT observations and one which does not. The value reported by Bothun et al. (1985a) is roughly 100 km s^{-1} larger than that found by all other observations. This, combined with the fact that the Bothun et al. W_{50} measurement is considerable smaller than their W_{20} measurement and is consistent with the other values found in the literature makes it likely that their high value for W_{20} is in error.

- **UGC 11017:** There are two published values for velocity width of UGC 11017, only one of which does not match that found in our survey. This measurement, which is lower by 40 km s^{-1} from the the other available measurements, was taken by Richter & Huchtmeier (1991) using the Arecibo telescope. Examining their profile shows the observation to be extremely low signal-to-noise, making their measured values suspect.

6.2. Total Flux Comparisons

For the flux measurements, the weighted average of the differences between our observations and those found in the literature (using the gain, beam, and pointing-corrected values in the literature) are zero regardless of the telescope used for the observations when comparing direct observations. However, the median difference between measurements in the literature and that found by us for non-Arecibo measurements differ by 20%, with the literature values being higher on average than our measurements (Figures 9 and 10).

To determine if the offset between the non-Arecibo measurements is due to many of the studies galaxies having H I emission extending beyond the Arecibo beam, we applied a beam dilution correction to all of the galaxies on our study. The beam dilution correction is based on Shostak's 1978 equation for the fraction of the total flux integral measured by a beam centered on a galaxy:

$$f \;=\; \frac{\sum_{j=1,2}\left[\frac{a_j\theta_j^2}{\left(1+\theta_j^2/\theta_B^2\right)^{1/2}\left(1+\theta_j^2/\theta_B^2\;cos^2 i\right)^{1/2}}\right]}{\sum_{j=1,2} a_j\theta_j^2}.$$

Here, $\theta_1 \sim D_{70}/1.1$ with $D_{70} = 1.2a$ (arcmin), $a_2 = -0.6a_1$ and $\theta_2 = 0.23\theta_1$ (Hewitt, Haynes, Giovanelli 1983). Additionally, the inclination is derived using the method described in Haynes & Giovanelli (1984) assuming galaxies are oblate spheroids:

$$cos^2 i \;=\; \left(r_i^2 \;-\; p^2\right)\left(1 \;-\; p^2\right)^{-1}$$

where $r_i = b/a$, $p = c/a$, a, b, and c are the spheroid's three axiis, and p is determined from the galaxy type. The result of applying this correction to the data is shown in Figure 10. Again the weighted difference between our observations with the corrected flux and those found in the literature are zero regardless of the telescope used for the observations. In this case, though, the median difference between measurements in the literature and that found by us for non-Arecibo measurements is lowered to 16%, with the literature values again being higher than our measurements (Figure 10). Consequently, while it seems likely that extended H I for some of the observed galaxies is responsible for the high differences in the median flux values between our measurements and those taken at telescopes with larger beams, the flux correction did not adequately (and possibly not accurately) correct for the extended H I.

To more thoroughly examine the flux differences found, we examined all galaxies with any published flux measurement differing from our measured value by at least $\pm$20%. Of the 26 galaxies which fall into this category, 25 were observed with the GBT. The last galaxy, UGC 12695, had VLA synthesis measurements which agree with our Arecibo observations, and no GBT follow-up was warranted. A complete listing of the 26 galaxies follows:

- 13 galaxies (UGC 0941, UGC 2885, UGC 3118, UGC 5160, UGC 5215, UGC 5218, UGC 6886, UGC 8503, UGC 9803, UGC 9450, UGC 11017, UGC 11627, UGC 12094) have values in the literature which vary significantly from our Arecibo measurements. In each case, follow-up observations with the GBT confirmed the Arecibo values.

- 7 galaxies (UGC 8091, UGC 9965, UGC 10351, UGC 10628, UGC 11461, UGC 11578, UGC 11992) have all flux values measured with a telescope with a larger beam, including our GBT measurements, to be larger than the values obtained at Arecibo (both by ourself and in the literature. As none of these galaxies have another source within 20′/1000 km s^{-1}, it is safe to assume that these objects have H I gas which extends well beyond the Arecibo beam, and that while our observations should be repeatable with the Arecibo telescope, the measured fluxes do not accurately reflect the total H I mass of the objects.

- Four other galaxies (UGC 2975, UGC 3476, UGC 4660, UGC 6464) with flux values in the literature discrepant from our Arecibo measurements were also observed with the GBT. Unfortunately, the follow-up observations did not reach a sufficient signal-to-noise to accurately determine the galaxies' fluxes with the GBT.

  The only literature values for UGC 2975 and UGC 6464 are from the pre-upgrade Arecibo telescope. The values found for UGC 6464 straddle those found with our observations, while the one value previously published for UGC 2975 is smaller than that found with our observations. In light of the extremely accurate fluxes found for all other sources in this survey, we are confident that our recent measurements of these objects are correct.

  UGC 4660 and UGC 3476 have literature values from the 300' Green Bank telescope which are larger than any Arecibo measurements taken of the galaxies. As a result, it is likely that the H I gas of these objects extends outside the Arecibo beam.

- UGC 12695 has 3 single dish observations and one interferometric (VLA) observation in the literature. The two pre-upgrade Arecibo measurements are higher than that found with our observations by 23–44%, while the Nançay measurement is 33% lower than ours. However, the published VLA value agrees with ours to within a few percent, again giving confidence that our measurements are accurate.

Compiling the above results shows that of the 108 galaxies observed for this project, only 9 have H I gas which extends beyond the Arecibo beam. As a result, measurements for these objects, while repeatable with the Arecibo 305m telescope, are not accurate representations of the total amount of neutral Hydrogen within the galaxies. Each of these objects is clearly marked in Table 1.

7. Conclusion

We have created a very reliable reference catalog of H I spectral line observations. Of the 108 galaxies observed, only 9 have measured fluxes indicating significant H I gas extending beyond the Arecibo beam. As a result, our catalog currently contains the most accurate H I line measurements and spectra available for the remaining 99 galaxies. This catalog should be an extremely useful, well-defined reference catalog for anyone interested in 21-cm spectral line work.

All data and results from this survey are available online at both http://www.naic.edu/∼astro/HIsurvey and http://www.gb.nrao.edu/∼koneil/HIsurvey.

REFERENCES

Baiesi-Pillastrini, G. & Palumbo, G. 1986 A&A 163, 1

Bicay, M. D. & Giovanelli, R. 1986, AJ, 91, 705

Bicay, M. D. & Giovanelli, R. 1986, AJ, 91, 732

Bothun, G. D., Beers, T. C., Mould, J. R., & Huchra, J. P. 1986, ApJ, 308, 510

Bothun, G. D., Aaronson, M., Schommer, B., Mould, J., Huchra, J., & Sullivan, W. T. 1985a, ApJS, 57, 423

Bothun, G. D., Aaronson, M., Schommer, B., Huchra, J., & Mould, J. 1984, ApJ, 278, 475

Davis, L. E. & Seaquist, E. R. 1983, ApJS, 53, 269

Fontanelli, P. 1984, A&A, 138, 85

Freudling, W., Haynes, M. P., & Giovanelli, R. 1988, AJ, 96, 1791

Ghigo, F., Maddalena, R., Balser, D., & Langston, G. 2001 Green Bank Telescope Commissioning Memo 10 *Gain and Efficiency at S-Band*. Available at http://wwwlocal.gb.nrao.edu/∼rmaddale/GBT/Commissioning/index.html

Ghosh, T. & Salter, C. 2001 *Arecibo Observatory Technical Memo 2001-02* http://www.naic.edu/∼astro/aotms/

Giovanardi, C. & Salpeter, E. E. 1985, ApJS, 58, 623

Giovanelli, R. & Haynes, M. P. 1993, AJ, 105, 1271

Giovanelli, R. & Haynes, M. P. 1989, AJ, 97, 633

Giovanelli, R., Myers, S. T., Roth, J., & Haynes, M. P. 1986, AJ, 92, 250

Giovanelli, R. & Haynes, M. P. 1985, ApJ, 292, 404

Giovanelli, R. & Haynes, M. P. 1985, AJ, 90, 2445

Haynes, M. P., Giovanelli, R., Herter, T., Vogt, N. P., Freudling, W., Maia, M. A. G., Salzer, J. J., & Wegner, G. 1997, AJ, 113, 1197

Haynes, M. P. & Giovanelli, R. 1984, AJ, 89, 758

Heiles, C. 2001 *Arecibo Technical and Operations Memo Series 2000-05* http://www.naic.edu/∼astro/aotms/

Helou, G., Salpeter, E. E., & Terzian, Y. 1982, AJ, 87, 1443

Hewitt, J. N., Haynes, M. P., & Giovanelli, R. 1983 AJ 88, 272

Hoffman, G. L., Williams, B. M., Lewis, B. M., Helou, G., & Salpeter, E. E. 1989, ApJS, 69, 65

Hoffman, G. L., Helou, G., Salpeter, E. E., & Sandage, A. 1985, ApJ, 289, L15

Huchtmeier, W. K. & Richter, O.-G 1989 A General Catalog of HI Observations of Galaxies. The Reference Catalog, XIX, 350 pp. 8 figs.. Springer-Verlag Berlin Heidelberg New York,

Huchtmeier, W. K. & Richter, O.-G. 1987, A&AS, 64, 111

Hunter, D. A. & Gallagher, J. S. 1985, AJ, 90, 1789

Impey, C. & Bothun, G. 1989, ApJ, 341, 89

Lewis, B. M., Helou, G., & Salpeter, E. E. 1985, ApJS, 59, 161

Lewis, B. M. 1987, ApJS, 63, 515

Lewis, B. M. 1984, ApJ, 285, 453

Nilson, P 1973 *Uppsala General Catalogue of Galaxies* Acta Universitatis Upsalienis, Nova Regiae Societatis Upsaliensis, Series

O'Neil, K., Bothun, G. D., & Schombert, J. 2000, AJ, 119, 136

Oosterloo, T. & Shostak, S. 1993, A&AS, 99, 379

Pantoja, C. A., Altschuler, D. R., Giovanardi, C., & Giovanelli, R. 1997, AJ, 113, 905

Peterson, S. D. 1979, ApJS, 40, 527

Richter, O.-G. & Huchtmeier, W. K. 1991, A&AS, 87, 425

Roelfsema, P. R. & Allen, R. J. 1985, A&A, 146, 213

Salter, C. *An Astronomer's Guide to the Arecibo 305-m Telescope* http://www2.naic.edu/∼astro/guide/

Schneider, S. E., Thuan, T. X., Mangum, J. G., & Miller, J. 1992, ApJS, 81, 5

Schneider, S. E., Thuan, T. X., Magri, C., & Wadiak, J. E. 1990, ApJS, 72, 245

Schneider, S. E., Helou, G., Salpeter, E. E., & Terzian, Y. 1986, AJ, 92, 742

Shostak, S. 1978 A&A 68, 321

Staveley-Smith, L. & Davies, R. D. 1987, MNRAS, 224, 953

Theureau, G., Bottinelli, L., Coudreau-Durand, N., Gouguenheim, L., Hallet, N., Loulergue, M., Paturel, G., & Teerikorpi, P. 1998, A&AS, 130, 333

Tifft, W.G. 1992 ApJS 79, 183

Tifft, W. G. & Cocke, W. J. 1988, ApJS, 67, 1

This 2-column preprint was prepared with the AAS LaTeX macros v5.2.

TABLE 1

FINAL RESULTS, BROKEN DOWN BY RESOLUTION

Name	RA	Dec	0.65 km s^{-1} Resolution			1.3 km s^{-1} Resolution			8.5 km s^{-1} Resolution			
	J2000		V_{HEL} [km s^{-1}]	Flux [Jy km s^{-1}]	W_{20} [km s^{-1}]	W_{50} [km s^{-1}]	Flux [Jy km s^{-1}]	W_{20} [km s^{-1}]	W_{50} [km s^{-1}]	Flux [Jy km s^{-1}]	W_{20} [km s^{-1}]	W_{50} [km s^{-1}]
UGC 199	00:20:51.7	12:51:22.0	1800 (3)	3.6 (0.2)	117 (7)	111 (3)	3.7 (0.2)	122 (4)	112 (3)	3.6 (0.2)	122 (4)	112 (4)
NGC 0257	00:48:01.6	08:17:48.0	5274 (2)	9.9 (0.5)	408 (11)	404 (1)	9.9 (0.5)	422 (10)	404 (3)	9.9 (0.5)	415 (4)	406 (4)
UGC 317	00:31:43.2	00:54:03.0	5361 (1)	1.1 (0.1)	37 (6)	33 (4)	1.1 (0.1)	44 (2)	35 (2)	1.1 (0.1)	44 (5)	38 (4)
UGC 628	01:00:51.9	19:28:33.0	5446 (5)	4.4 (0.2)	241 (4)	232 (5)	4.4 (0.2)	243 (7)	234 (3)	4.4 (0.2)	244 (4)	234 (4)
UGC 941	01:23:32.4	06:57:38.0	2729 (4)	3.6 (0.2)	87 (8)	85 (7)	3.6 (0.2)	104 (4)	80 (3)	3.6 (0.2)	89 (4)	82 (4)
UGC 989	01:25:29.6	07:33:41.0	2785 (2)	5.4 (0.3)	161 (11)	153 (4)	5.4 (0.3)	164 (5)	154 (3)	5.4 (0.3)	165 (4)	154 (4)
UGC 1085	01:31:18.8	07:47:16.0	651 (3)	2.1 (0.1)	60 (7)	55 (2)	2.1 (0.1)	74 (5)	56 (6)	2.1 (0.1)	65 (4)	60 (4)
UGC 1246	01:47:00.7	12:24:21.0	803 (1)	8.6 (0.4)	113 (3)	99 (2)	8.7 (0.4)	117 (2)	100 (1)	8.6 (0.4)	113 (4)	103 (4)
UGC 1519	02:02:16.8	19:10:48.0	2346 (3)	2.5 (0.1)	129 (3)	121 (4)	2.4 (0.1)	135 (2)	122 (4)	2.5 (0.1)	135 (4)	125 (4)
UGC 2008	02:32:32.2	31:36:35.0	5043 (4)	2.7 (0.1)	139 (8)	128 (8)	2.7 (0.1)	150 (9)	130 (4)	2.7 (0.1)	143 (4)	133 (4)
UGC 2339	02:51:23.6	16:02:30.0	16467 (11)	4.5 (0.2)	497 (3)	469 (3)	4.5 (0.2)	500 (16)	472 (17)	4.5 (0.2)	497 (7)	475 (7)
UGC 2432	02:57:26.7	10:08:12.0	758 (1)	5.9 (0.3)	114 (1)	105 (0)	5.9 (0.3)	115 (1)	104 (1)	5.9 (0.3)	116 (4)	105 (4)
AC HVC	-753 (1)	...	...	...	0.7 (0.1)	42 (1)	36 (2)	...	...	...		
UGC 2602	03:14:10.1	16:29:08.0	10092 (8)	6.0 (0.3)	302 (17)	290 (11)	5.9 (0.3)	307 (16)	290 (4)	5.9 (0.3)	302 (7)	290 (4)
UGC 2809	03:39:33.2	19:47:03.0	1287 (1)	9.9 (0.5)	154 (2)	144 (1)	9.9 (0.5)	156 (2)	144 (1)	9.9 (0.5)	156 (4)	146 (4)
UGC 2885	03:53:02.4	35:35:22.0	5803 (7)	19.2 (1.0)	580 (4)	567 (8)	19.0 (1.0)	591 (7)	567 (3)	19.2 (1.0)	585 (4)	572 (4)
UGC 2905	03:57:00.1	16:31:21.0	295 (1)	4.1 (0.2)	75 (7)	65 (3)	4.0 (0.2)	82 (1)	68 (1)	4.1 (0.2)	75 (4)	68 (4)
UGC 2922	04:00:46.0	17:35:00.0	5220 (2)	4.6 (0.2)	369 (4)	364 (7)	4.7 (0.2)	380 (7)	361 (3)	4.6 (0.2)	375 (5)	364 (5)
UGC 2975	04:11:00.4	26:36:46.0	19945 (17)	2.0 (0.1)	316 (10)	282 (2)	2.0 (0.1)	327 (3)	284 (2)	2.0 (0.1)	325 (11)	285 (16)
UGC 3044	04:26:50.0	29:56:52.0	5231 (7)	2.7 (0.1)	248 (8)	240 (10)	2.6 (0.1)	254 (6)	240 (6)	2.7 (0.1)	250 (5)	240 (4)
UGC 3118	04:38:59.0	05:37:11.0	8314 (5)	1.6 (0.1)	78 (4)	74 (1)	1.6 (0.1)	99 (7)	75 (1)	1.6 (0.1)	89 (11)	75 (4)
UGC 3169	04:47:45.0	09:35:43.0	8800 (8)	3.0 (0.2)	378 (0)	382 (0)	3.0 (0.2)	400 (1)	370 (1)	2.9 (0.1)	399 (4)	374 (4)
UGC 3247	05:06:38.0	08:40:27.0	3365 (7)	5.2 (0.3)	220 (0)	208 (0)	5.1 (0.3)	239 (1)	177 (1)	5.2 (0.3)	223 (4)	209 (4)
UGC 3296	05:21:21.8	04:53:16.0	4267 (3)	8.6 (0.4)	342 (0)	332 (0)	8.8 (0.4)	361 (1)	335 (1)	8.6 (0.4)	346 (4)	333 (4)
UGC 3330	05:36:46.9	14:25:21.0	5238 (3)	4.6 (0.2)	211 (11)	189 (18)	4.5 (0.2)	216 (7)	185 (11)	4.6 (0.2)	212 (7)	188 (4)
UGC 3476†	06:30:29.2	33:18:07.0	472 (5)	7.4 (0.4)	128 (13)	104 (8)	7.3 (0.4)	150 (3)	106 (5)	7.4 (0.4)	130 (4)	119 (4)
UGC 3564	06:50:36.2	16:21:20.0	2546 (0)	5.6 (0.3)	97 (0)	86 (1)	5.6 (0.3)	103 (1)	90 (1)	5.6 (0.3)	100 (4)	91 (4)
UGC 3582	06:53:00.3	12:11:17.0	8392 (10)	2.8 (0.1)	177 (28)	165 (23)	2.8 (0.1)	189 (18)	164 (2)	2.8 (0.1)	183 (11)	166 (4)
UGC 3621	06:59:04.4	14:17:42.0	2335 (2)	9.6 (0.5)	176 (1)	165 (2)	9.6 (0.5)	177 (3)	164 (1)	9.6 (0.5)	177 (4)	166 (4)
UGC 3755	07:13:51.5	10:31:19.0	318 (4)	8.2 (0.4)	67 (7)	77 (6)	8.1 (0.4)	111 (3)	79 (5)	8.2 (0.4)	71 (4)	80 (4)
UGC 3767	07:14:47.7	06:46:50.0	5807 (4)	4.0 (0.2)	261 (4)	254 (3)	4.0 (0.2)	264 (10)	254 (6)	4.0 (0.2)	266 (4)	257 (4)
CAP 0718+06	07:21:00.2	06:18:19.0	11140 (6)	1.4 (0.1)	207 (10)	207 (11)	1.4 (0.1)	209 (11)	192 (11)	1.4 (0.1)	211 (16)	195 (8)
UGC 3946	07:37:59.7	03:18:58.0	1198 (6)	12.0 (0.6)	123 (13)	112 (4)	12.1 (0.6)	143 (9)	114 (1)	12.0 (0.6)	127 (4)	113 (4)
UGC 4117	07:57:26.0	35:56:21.0	773 (1)	4.1 (0.2)	80 (5)	73 (2)	4.1 (0.2)	88 (1)	76 (1)	4.1 (0.2)	85 (4)	76 (4)
UGC 4131	07:59:11.6	31:48:28.0	17728 (24)	3.4 (0.2)	464 (14)	448 (19)	3.4 (0.2)	467 (32)	451 (25)	3.4 (0.2)	466 (16)	448 (25)
UGC 4180	08:02:36.5	27:26:15.0	5229 (2)	5.3 (0.3)	354 (2)	347 (9)	5.2 (0.3)	356 (4)	348 (5)	5.3 (0.3)	359 (4)	350 (4)
UGC 4385	08:23:52.0	14:45:07.0	1967 (5)	6.6 (0.3)	185 (7)	168 (2)	6.6 (0.3)	190 (9)	169 (5)	6.6 (0.3)	188 (4)	170 (4)
LSBC F704-V01	08:24:51.7	09:13:29.0	6018 (5)	2.0 (0.1)	135 (10)	130 (13)	2.0 (0.1)	141 (5)	131 (5)	2.0 (0.1)	139 (4)	132 (4)
UGC 4660†	08:54:24.2	34:33:20.0	2202 (2)	6.0 (0.3)	77 (4)	69 (2)	6.0 (0.3)	80 (2)	69 (1)	6.0 (0.3)	80 (4)	73 (4)
UGC 4780	09:06:39.4	19:20:10.0	3287 (6)	8.1 (0.4)	164 (15)	139 (5)	8.2 (0.4)	169 (2)	140 (1)	8.1 (0.4)	165 (4)	142 (4)
UGC 4955	09:20:19.3	25:16:25.0	6463 (4)	2.1 (0.1)	209 (0)	202 (0)	2.1 (0.1)	214 (1)	206 (1)	2.1 (0.1)	217 (4)	207 (4)
UGC 5030	09:26:36.2	07:57:15.0	2153 (2)	3.4 (0.2)	300 (3)	295 (7)	3.3 (0.2)	305 (12)	295 (11)	3.4 (0.2)	306 (8)	297 (4)
UGC 5160	09:40:41.7	11:53:18.0	6660 (13)	2.9 (0.1)	399 (21)	398 (25)	2.8 (0.1)	402 (25)	390 (24)	2.9 (0.1)	405 (19)	397 (8)

TABLE 1—*Continued*

Name	RA	Dec	0.65 km s^{-1} Resolution			1.3 km s^{-1} Resolution			8.5 km s^{-1} Resolution			
	J2000		V_{HEL} [km s^{-1}]	Flux [Jy km s^{-1}]	W_{20} [km s^{-1}]	W_{50} [km s^{-1}]	Flux [Jy km s^{-1}]	W_{20} [km s^{-1}]	W_{50} [km s^{-1}]	Flux [Jy km s^{-1}]	W_{20} [km s^{-1}]	W_{50} [km s^{-1}]
UGC 5215	09:45:14.3	09:06:35.0	5485 (1)	6.8 (0.3)	420 (0)	418 (0)	6.8 (0.3)	425 (1)	416 (1)	6.8 (0.3)	424 (4)	417 (4)
UGC 5218	09:45:30.2	06:22:37.0	3088 (1)	6.7 (0.3)	195 (4)	185 (2)	6.7 (0.3)	200 (1)	186 (1)	6.7 (0.3)	199 (4)	188 (4)
UGC 5326	09:55:24.6	33:15:45.0	1412 (8)	4.3 (0.2)	131 (6)	112 (6)	4.3 (0.2)	128 (8)	111 (4)	4.3 (0.2)	132 (11)	115 (4)
UGC 5358	09:58:47.2	11:23:19.0	2914 (1)	4.4 (0.2)	216 (0)	203 (0)	4.5 (0.2)	222 (1)	204 (1)	4.4 (0.2)	218 (4)	207 (4)
UGC 5440	10:05:35.9	04:16:45.0	18958 (14)	3.0 (0.2)	537 (34)	537 (35)	3.1 (0.2)	513 (19)	484 (20)	2.9 (0.1)	508 (13)	498 (13)
UGC 5629	10:24:12.8	21:03:01.0	1238 (1)	2.9 (0.1)	126 (4)	116 (4)	2.8 (0.1)	129 (3)	116 (4)	2.9 (0.1)	129 (4)	118 (4)
UGC 5651	10:26:25.6	17:30:38.0	5567 (2)	5.3 (0.3)	224 (10)	218 (1)	5.2 (0.3)	234 (4)	219 (1)	5.2 (0.3)	231 (4)	221 (4)
UGC 5852	10:44:12.1	06:45:33.0	6174 (4)	11.2 (0.6)	380 (23)	362 (4)	11.2 (0.6)	385 (8)	363 (4)	11.2 (0.6)	379 (7)	364 (4)
UGC 6018	10:54:05.8	20:38:41.0	1294 (2)	1.9 (0.1)	61 (11)	57 (6)	1.9 (0.1)	70 (17)	57 (3)	1.9 (0.1)	69 (5)	61 (4)
UGC 6421	11:24:25.7	27:27:23.0	1502 (1)	7.9 (0.4)	175 (2)	169 (0)	8.0 (0.4)	181 (5)	170 (1)	7.9 (0.4)	178 (4)	171 (4)
UGC 6464	11:28:09.3	16:55:14.0	1075 (5)	3.5 (0.2)	154 (1)	141 (8)	3.4 (0.2)	168 (5)	144 (10)	3.6 (0.2)	169 (8)	148 (4)
UGC 6476	11:28:36.0	23:24:15.0	7328 (9)	3.7 (0.2)	321 (4)	319 (1)	3.6 (0.2)	328 (1)	319 (5)	3.7 (0.2)	326 (4)	319 (5)
[OBC97] U01-4	11:38:25.7	17:05:03.0	3452 (3)	1.8 (0.1)	197 (0)	177 (3)	1.8 (0.1)	192 (7)	176 (10)	1.8 (0.1)	191 (4)	182 (4)
UGC 6872	11:53:50.9	33:21:55.0	3203 (5)	5.7 (0.3)	216 (6)	198 (30)	5.7 (0.3)	220 (11)	198 (11)	5.6 (0.3)	221 (29)	201 (7)
UGC 6886	11:55:11.3	06:10:09.0	6973 (20)	4.6 (0.2)	384 (11)	383 (22)	4.6 (0.2)	404 (50)	377 (1)	4.6 (0.2)	395 (7)	383 (7)
UGC 7302	12:16:49.4	30:16:13.0	3838 (2)	3.9 (0.2)	91 (6)	82 (1)	3.9 (0.2)	95 (5)	83 (1)	3.9 (0.2)	93 (4)	84 (4)
UGC 7666	12:31:37.7	14:51:38.0	2556 (10)	2.2 (0.1)	129 (18)	111 (2)	2.3 (0.1)	151 (14)	116 (7)	2.2 (0.1)	138 (8)	117 (4)
Malin 1	12:36:59.2	14:19:50.0	24768 (17)	2.1 (0.1)	417 (16)	396 (14)	2.1 (0.1)	514 (10)	331 (8)	2.1 (0.1)	372 (7)	332 (5)
UGC 7976	12:49:15.8	04:39:27.0	2666 (1)	6.4 (0.3)	92 (11)	80 (1)	6.4 (0.3)	94 (1)	81 (1)	6.4 (0.3)	92 (4)	82 (4)
UGC 8091‡	12:58:40.0	14:13:00.0	213 (0)	7.0 (0.4)	44 (2)	44 (1)	7.0 (0.4)	55 (2)	44 (2)	7.0 (0.4)	45 (4)	45 (4)
UGC 8249	13:10:26.5	24:55:15.0	2541 (1)	7.5 (0.4)	187 (14)	178 (2)	7.4 (0.4)	189 (5)	179 (2)	7.5 (0.4)	192 (4)	181 (4)
UGC 8503	13:30:44.9	32:45:38.0	4676 (4)	3.7 (0.2)	72 (6)	65 (2)	3.7 (0.2)	83 (8)	69 (2)	3.7 (0.2)	75 (5)	71 (4)
UGC 8516	13:31:52.5	20:00:01.0	1020 (3)	3.6 (0.2)	125 (11)	114 (2)	3.7 (0.2)	126 (12)	115 (2)	3.7 (0.2)	128 (4)	115 (4)
UGC 8896	13:58:38.5	07:12:58.0	4401 (9)	5.1 (0.3)	303 (18)	291 (20)	5.1 (0.3)	312 (21)	298 (16)	5.1 (0.3)	311 (4)	298 (4)
UGC 8904	13:58:51.0	26:06:24.0	9773 (3)	3.5 (0.2)	300 (0)	285 (0)	3.6 (0.2)	296 (1)	272 (1)	3.6 (0.2)	290 (4)	278 (4)
UGC 9007	14:05:06.0	09:20:21.0	4618 (4)	1.4 (0.1)	59 (6)	54 (4)	1.4 (0.1)	66 (7)	56 (1)	1.4 (0.1)	63 (4)	57 (4)
UGC 9134	14:16:35.2	09:59:09.0	11158 (19)	4.1 (0.2)	350 (30)	334 (28)	4.0 (0.2)	359 (25)	339 (12)	4.0 (0.2)	356 (21)	337 (4)
UGC 9450	14:39:45.4	23:23:50.0	4471 (9)	2.4 (0.1)	221 (13)	205 (13)	2.4 (0.1)	223 (13)	209 (10)	2.4 (0.1)	214 (5)	207 (4)
UGC 9535	14:48:42.5	12:27:25.0	1792 (1)	8.6 (0.4)	200 (5)	192 (1)	8.7 (0.4)	205 (1)	192 (1)	8.7 (0.4)	202 (4)	194 (4)
UGC 9698	15:05:27.2	23:41:18.0	4853 (6)	2.7 (0.1)	198 (21)	172 (10)	2.6 (0.1)	207 (19)	173 (20)	2.7 (0.1)	203 (9)	177 (4)
UGC 9803	15:17:17.8	29:24:00.0	5257 (2)	1.5 (0.1)	82 (1)	72 (2)	1.5 (0.1)	80 (7)	70 (5)	1.6 (0.1)	88 (7)	73 (4)
UGC 9901	15:34:27.0	12:16:12.0	3160 (1)	5.9 (0.3)	246 (3)	237 (2)	5.9 (0.3)	247 (3)	234 (3)	5.9 (0.3)	246 (4)	236 (4)
UGC 9965‡	15:40:06.6	20:40:50.0	4524 (11)	4.7 (0.2)	133 (20)	113 (31)	4.8 (0.2)	153 (21)	114 (36)	4.7 (0.2)	125 (14)	118 (4)
UGC 9979	15:42:19.3	00:28:31.0	1961 (3)	4.8 (0.2)	137 (4)	126 (1)	4.8 (0.2)	144 (7)	132 (3)	4.8 (0.2)	144 (4)	129 (4)
UGC 10042	15:48:57.2	07:13:18.0	4224 (5)	4.6 (0.2)	342 (5)	335 (12)	4.6 (0.2)	350 (12)	336 (1)	4.6 (0.2)	348 (4)	340 (4)
UGC 10243	16:10:29.6	19:57:15.0	7937 (2)	4.6 (0.2)	165 (5)	146 (6)	4.5 (0.2)	162 (5)	146 (5)	4.6 (0.2)	165 (4)	147 (6)
UGC 10351‡	16:21:28.2	28:38:25.0	891 (1)	6.3 (0.3)	70 (2)	66 (0)	6.4 (0.3)	79 (1)	65 (1)	6.3 (0.3)	71 (4)	67 (4)
UGC 10384	16:26:46.7	11:34:49.0	4966 (5)	7.0 (0.4)	384 (9)	370 (3)	7.0 (0.4)	386 (22)	373 (3)	7.0 (0.3)	383 (6)	371 (4)
UGC 10628‡	16:58:08.6	22:59:06.0	2980 (2)	5.0 (0.3)	259 (1)	250 (3)	5.1 (0.3)	261 (7)	247 (1)	5.0 (0.3)	260 (4)	252 (4)
UGC 10721	17:08:25.5	25:31:02.0	2920 (5)	5.3 (0.3)	286 (11)	273 (12)	5.3 (0.3)	298 (17)	276 (8)	5.3 (0.3)	292 (4)	279 (4)
UGC 10747	17:11:59.7	23:22:48.0	8821 (4)	3.3 (0.2)	317 (0)	317 (0)	3.3 (0.2)	340 (1)	313 (1)	3.3 (0.2)	327 (4)	322 (4)
UGC 10901	17:33:54.0	05:28:34.0	2834 (1)	9.2 (0.5)	190 (0)	184 (0)	9.2 (0.5)	193 (1)	185 (1)	9.2 (0.5)	195 (4)	186 (4)
UGC 11017	17:52:08.6	29:51:41.0	4644 (0)	3.9 (0.2)	183 (0)	167 (0)	3.9 (0.2)	187 (1)	173 (1)	3.9 (0.2)	186 (4)	174 (4)

TABLE 1—*Continued*

Name	RA	Dec	0.65 km s^{-1} Resolution			1.3 km s^{-1} Resolution			8.5 km s^{-1} Resolution			
	J2000		V_{HEL} [km s^{-1}]	Flux [Jy km s^{-1}]	W_{20} [km s^{-1}]	W_{50} [km s^{-1}]	Flux [Jy km s^{-1}]	W_{20} [km s^{-1}]	W_{50} [km s^{-1}]	Flux [Jy km s^{-1}]	W_{20} [km s^{-1}]	W_{50} [km s^{-1}]
UGC 11120	18:07:02.2	20:29:17.0	2242 (6)	3.6 (0.2)	179 (0)	169 (10)	3.6 (0.2)	178 (13)	167 (2)	3.6 (0.2)	182 (4)	170 (4)
UGC 11285	18:35:14.3	22:29:58.0	4501 (4)	5.3 (0.3)	306 (6)	300 (8)	5.4 (0.3)	315 (9)	303 (4)	5.3 (0.3)	314 (13)	304 (4)
UGC 11362	18:49:56.0	23:15:16.0	4205 (2)	3.7 (0.2)	197 (20)	191 (11)	3.7 (0.2)	207 (14)	192 (1)	3.7 (0.2)	204 (11)	194 (4)
UGC 11461‡	19:39:09.1	08:48:37.0	3122 (4)	6.6 (0.3)	322 (37)	298 (37)	6.6 (0.3)	326 (10)	299 (8)	6.6 (0.3)	324 (8)	302 (4)
UGC 11482	19:49:20.1	07:09:35.0	3160 (3)	8.3 (0.4)	289 (4)	280 (8)	8.4 (0.4)	293 (7)	278 (1)	8.3 (0.4)	290 (4)	281 (4)
UGC 11504	20:02:25.2	07:46:33.0	5620 (2)	3.1 (0.2)	150 (6)	138 (5)	3.1 (0.2)	160 (7)	142 (5)	3.2 (0.2)	163 (7)	147 (4)
UGC 11578‡	20:30:42.7	09:11:25.0	4601 (1)	8.7 (0.4)	99 (1)	88 (1)	8.7 (0.4)	104 (2)	88 (1)	8.7 (0.4)	100 (4)	90 (4)
UGC 11624	20:46:15.8	06:42:43.0	4831 (2)	3.2 (0.2)	218 (7)	209 (8)	3.2 (0.2)	219 (4)	206 (1)	3.2 (0.2)	219 (4)	210 (4)
UGC 11627	20:46:48.9	05:38:47.0	4864 (2)	2.3 (0.1)	126 (9)	118 (6)	2.3 (0.1)	132 (10)	117 (7)	2.3 (0.1)	134 (4)	119 (4)
UGC 11655	20:57:49.4	25:38:15.0	4754 (4)	3.8 (0.2)	266 (6)	259 (9)	3.8 (0.2)	274 (10)	262 (7)	3.8 (0.2)	275 (4)	264 (4)
UGC 11708	21:14:56.0	02:50:05.0	4164 (2)	7.5 (0.4)	292 (4)	282 (7)	7.4 (0.4)	301 (4)	283 (2)	7.5 (0.4)	296 (4)	285 (4)
UGC 11774	21:36:10.6	17:03:40.0	6875 (5)	3.7 (0.2)	235 (11)	232 (10)	3.7 (0.2)	241 (9)	232 (1)	3.6 (0.2)	238 (4)	231 (4)
UGC 11849	21:55:40.2	24:53:51.0	5840 (3)	4.3 (0.2)	357 (15)	347 (12)	4.3 (0.2)	359 (9)	348 (5)	4.3 (0.2)	358 (7)	349 (4)
UGC 11926	22:09:31.1	18:40:54.0	1652 (1)	5.2 (0.3)	110 (3)	100 (1)	5.2 (0.3)	111 (4)	100 (1)	5.2 (0.3)	112 (4)	102 (4)
UGC 11992‡	22:20:47.4	14:14:05.0	3592 (1)	5.3 (0.3)	174 (8)	169 (2)	5.3 (0.3)	178 (1)	169 (2)	5.3 (0.3)	179 (4)	171 (4)
UGC 12094	22:34:46.0	22:33:48.0	7607 (9)	1.8 (0.1)	59 (16)	59 (32)	1.7 (0.1)	86 (13)	55 (4)	1.8 (0.1)	66 (16)	71 (4)
UGC 12158	22:42:10.5	19:59:49.0	9289 (5)	4.3 (0.2)	178 (7)	160 (7)	4.3 (0.2)	187 (6)	164 (4)	4.3 (0.2)	184 (4)	164 (4)
UGC 12388	23:08:30.2	12:49:49.0	4584 (3)	6.3 (0.3)	272 (14)	266 (12)	6.2 (0.3)	281 (10)	266 (3)	6.3 (0.3)	277 (6)	269 (4)
[OBC97] P02-3	23:16:59.0	07:52:19.0	3178 (3)	1.9 (0.1)	109 (5)	103 (7)	1.8 (0.1)	108 (5)	99 (2)	1.9 (0.1)	112 (6)	103 (4)
UGC 12537	23:21:07.9	29:32:58.0	6112 (6)	3.6 (0.2)	445 (16)	445 (12)	3.5 (0.2)	452 (19)	448 (11)	3.6 (0.2)	452 (5)	448 (4)
[OBC97] P07-1	23:22:58.5	07:40:20.0	3472 (6)	1.4 (0.1)	171 (20)	162 (24)	1.4 (0.1)	171 (10)	165 (6)	1.4 (0.1)	176 (6)	168 (6)
UGC 12624	23:29:07.6	21:33:51.0	3516 (2)	3.5 (0.2)	194 (1)	183 (3)	3.5 (0.2)	201 (4)	186 (2)	3.5 (0.2)	198 (7)	187 (4)
UGC 12695	23:36:02.2	12:52:32.0	6185 (2)	4.2 (0.2)	85 (8)	78 (4)	4.2 (0.2)	95 (11)	78 (4)	4.2 (0.2)	89 (5)	80 (4)
UGC 12910	00:01:28.3	05:23:22.0	3948 (4)	2.8 (0.1)	74 (9)	63 (3)	2.8 (0.1)	83 (4)	66 (4)	2.8 (0.1)	77 (4)	67 (4)

NOTE.—†This galaxy may have H I extending beyond the Arecibo beam, resulting in the flux measurements reported here being too low. No GBT follow-up results are availale. See Section 6.2 for more details.
‡This galaxy has H I extending beyond the Arecibo beam, resulting in the flux measurements reported here being too low. The results from the GBT observations (Table 2) are more reliable. See Section 6.2 for more details.

TABLE 2
RESULTS FROM GBT OBSERVATONS

Name	V_{HEL} [km s^{-1}]	Flux [Jy km s^{-1}]	rms [Jy]	W_{20} [km s^{-1}]	W_{50} [km s^{-1}]
UGC 941	2729 (8)	3.7 (0.4)	3.3	95 (16)	74 (16)
UGC 2885	5799 (8)	20.7 (2.1)	4.5	593 (16)	576 (16)
UGC 2922	5210 (8)	5.0 (0.5)	3.6	411 (16)	390 (16)
UGC 3118†	8297 (8)	1.8 (0.2)	2.9	86 (16)	78 (16)
UGC 5160	6653 (8)	2.9 (0.3)	1.2	405 (16)	387 (16)
UGC 5215	5475 (8)	7.5 (0.8)	1.5	440 (16)	420 (16)
UGC 5218	3147 (8)	7.7 (0.8)	3.0	260 (16)	192 (16)
UGC 6886	6984 (8)	4.8 (0.5)	1.9	388 (16)	371 (16)
UGC 8091	213 (8)	8.8 (0.9)	3.5	53 (16)	41 (16)
UGC 8249	2540 (8)	9.0 (0.9)	3.1	191 (16)	181 (16)
UGC 8503	4674 (8)	2.3 (0.3)	8.3	85 (16)	78 (16)
UGC 9007	4617 (8)	1.5 (0.2)	2.9	63 (16)	52 (16)
UGC 9450	4487 (8)	2.6 (0.3)	2.2	206 (16)	197 (16)
UGC 9803	5259 (8)	1.5 (0.2)	2.7	78 (16)	69 (16)
UGC 9965	4526 (8)	5.3 (0.5)	3.1	126 (16)	101 (16)
UGC 10351	891 (8)	9.0 (0.9)	2.3	78 (16)	63 (16)
UGC 10628	2979 (8)	5.8 (0.6)	2.1	273 (16)	247 (16)
UGC 11017	4648 (8)	4.4 (0.4)	2.2	197 (16)	182 (16)
UGC 11461	3125 (8)	8.1 (0.8)	2.5	319 (16)	303 (16)
UGC 11578	4602 (8)	10.9 (1.1)	3.0	103 (16)	86 (16)
UGC 11627	4861 (8)	2.4 (0.2)	2.1	114 (16)	113 (16)
UGC 11992	3597 (8)	6.2 (0.6)	2.4	185 (16)	172 (16)
UGC 12094†	7589 (8)	1.6 (0.2)	3.6	56 (16)	44 (16)

NOTE.—†The heliocentric velocity found by the GBT for this galaxy is off by $\sim$17 km s^{-1} due to an instrumental error.

TABLE 3

LITERATURE VALUES

Name	Flux [Jy km s^{-1}]	W_{20} [km s^{-1}]	W_{50} [km s^{-1}]	v_{HEL} [km s^{-1}]	Tel.[1]	Refs.
UGC 199	3.13 (0.2)	122 (3)	106 (2)	1803 (4)	A	a
NGC 257	12.5 (1.2^2)	426 (4)	402 (4)	5278 (5)	A	b
NGC 257	11.7 (1.2^2)	437 (4)	394 (4)	5270 (5)	A	c
UGC 317	0.970 (0.3)	47 (7)	30 (4)	5264 (5)	A	a
UGC 317	0.990 (0.1^2)	41 (9)	27 (6)	5361 (5)	G	d
UGC 628	4.52 (0.5^2)	239 (8^3)	222 (8^3)	5447 (8^3)	A	e
UGC 628	4.73 (0.3)	251 (6)	229 (4)	5446 (4)	A	a
UGC 628	4.20 (1.1)	237 (10)	224 (7)	5443 (5)	G	d
UGC 941	2.02 (0.2)	88 (8)	47 (5)	2726 (5)	A	a
UGC 989	5.71 (0.3)	166 (4)	146 (2)	5107 (5)	A	a
UGC 1085	1.68 (0.2)	58 (3)	38 (2)	652 (4)	A	a
UGC 1246	7.35 (0.2)	109 (2)	82 (2)	804 (4)	A	a
UGC 1519	2.27 (0.2)	132 (4)	117 (3)	2346 (4)	A	a
UGC 1519	2.13 (0.2^2)	123 (8^3)	111 (8^3)	2346 (8^3)	A	e
UGC 2008	1.93 (0.3)	124 (5)	109 (8)	5041 (5)	A	a
UGC 2008	2.69 (0.5)	147 (15^3)	127 (15^3)	5042 (15^3)	A	f
UGC 2339	2.17 (0.2^2)	334 (15^3)	325 (15^3)	4821 (15^3)	A	f
UGC 2339	4.46 (0.4^2)	478 (8^3)	457 (8^3)	16469 (8^3)	A	e
UGC 2339	4.33 (0.4^2)	457 (8^3)	...	16469 (8^3)	A	g
UGC 2432	5.67 (0.3)	107 (3)	88 (2)	764 (4^3)	A	a
UGC 2602	7.01 (0.7^2)	298 (8^3)	276 (8^3)	10099 (8^3)	A	e
UGC 2602	5.10 (0.8)	305 (25)	267 (17)	10098 (8)	N	h
UGC 2809	9.29 (0.2)	155 (2)	131 (1)	1293 (4)	A	a
UGC 2885	25.2 (2.5^2)	629 (34^3)	583 (34^3)	5794 (34^3)	W	i
UGC 2885	34.2 (3.4)	595 (4)	550 (4)	5801 (4)	J	j
UGC 2885	17.3 (1.7^2)	581 (4)	556 (4)	5802 (15^3)	A	k
UGC 2885	32.7 (3.3^2)	607 (4)	...	5801 (2)	G	l
UGC 2905	4.67 (0.5^2)	71 (8^3)	47 (8^3)	293 (8^3)	A	e
UGC 2905	4.47 (0.1)	71 (1)	48 (1)	292 (4)	A	a
UGC 2922	5.12 (0.5^2)	370 (8^3)	351 (8^3)	5215 (8^3)	A	e
UGC 2975	2.41 (0.2^2)	312 (3)	280 (3)	19937 (8^3)	A	m
UGC 3044	2.20 (0.3)	246 (9)	228 (5)	5234 (5)	A	a
UGC 3118	1.72 (0.2)	89 (8)	55 (5)	8310 (5)	A	a
UGC 3118	0.620 (0.4)	65 (13)	51 (9)	8316 (6)	G	d
UGC 3169	2.79 (0.3^2)	373 (3)	358 (3)	8788 (3)	A	n
UGC 3247	5.99 (0.6^2)	196 (2)	137 (3)	3369 (3)	A	n
UGC 3247	5.15 (0.5^2)	213 (4)	143 (4)	3373 (4)	A	o
UGC 3296	10.5 (1.1^2)	335 (3)	315 (3)	4269 (3)	A	p
UGC 3296	7.56 (0.8^2)	348 (4)	318 (4)	4264 (15^3)	A	k
UGC 3330	5.22 (0.5^2)	204 (3)	163 (3)	5234 (3)	A	n
UGC 3330	4.52 (0.5^2)	202 (4)	170 (4)	5239 (4)	A	o
UGC 3476	12.3 (0.6)	141 (9)	83 (5)	469 (5)	G	d
UGC 3476	7.33 (0.3)	117 (6)	70 (4)	469 (4)	A	a
UGC 3564	6.26 (0.6^2)	94 (3)	79 (3)	2548 (3)	A	n
UGC 3564	5.47 (0.2)	97 (2)	75 (1)	2548 (4)	A	a
UGC 3582	2.94 (0.3^2)	171 (3)	152 (3)	839 (3)	A	n
UGC 3621	9.56 (0.5)	177 (4)	159 (2)	2337 (4)	A	a
UGC 3621	9.59 (1.0^2)	173 (3)	158 (3)	2337 (3)	A	n
UGC 3621	10.3 (1.0^2)	172 (4)	156 (4)	2336 (4)	A	o
UGC 3755	8.36 (0.8^2)	84 (3)	43 (3)	315 (3)	A	n
UGC 3755	8.49 (0.3)	70 (2)	37 (1)	314 (4)	A	a
UGC 3767	4.49 (0.4^2)	264 (3)	246 (3)	5809 (3)	A	n
UGC 3767	3.38 (0.3)	273 (7)	254 (5)	5806 (5)	A	a
UGC 3946	11.2 (0.3)	108 (3)	76 (2)	1195 (4)	A	a
UGC 3946	11.8 (1.2^2)	112 (3)	79 (3)	1194 (3)	A	n
UGC 3946	14.3 (1.4^2)	126 (4)	...	1199 (1)	G	l
UGC 4117	3.55 (0.4)	80 (6)	59 (4)	775 (4)	A	a
UGC 4180	6.16 (0.6^2)	343 (8^3)	330 (8^3)	5225 (8^3)	A	g
UGC 4180	5.18 (0.5)	...	347 (4^3)	5223 (4^3)	A	q
UGC 4180	5.50 (0.6^2)	358 (4)	333 (4)	5231 (4)	A	k
UGC 4385	6.60 (0.7^2)	...	171 (5)	1969 (8^3)	A	r
UGC 4660	6.23 (0.6^2)	88 (3)	61 (3)	2203 (3)	A	n

TABLE 3—*Continued*

Name	Flux [Jy km s^{-1}]	W_{20} [km s^{-1}]	W_{50} [km s^{-1}]	v_{HEL} [km s^{-1}]	Tel.[1]	Refs.
UGC 4660	5.67 (0.6^2)	69 (4)	57 (4)	2201 (4)	A	r
UGC 4660	7.30 (0.2)	75 (4)	···	2205 (2)	G	l
UGC 4780	7.54 (0.2)	167 (4)	128 (2)	3292 (4)	A	a
UGC 4780	9.13 (0.9^2)	147 (3)	124 (3)	3283 (3)	A	n
UGC 4955	1.98 (0.2)	225 (12)	199 (8)	6462 (8)	A	a
UGC 5030	2.94 (0.3^2)	300 (3)	286 (3)	2148 (···)	A	n
UGC 5030	3.72 (0.4^2)	307 (4)	285 (4)	2150 (15^3)	A	k
UGC 5160	4.27 (0.4^2)	416 (4)	381 (4)	6663 (15^3)	A	k
UGC 5215	9.05 (0.9^2)	427 (4)	404 (4)	5484 (15^3)	A	k
UGC 5218	7.01 (0.7^2)	194 (3)	183 (3)	3085 (3)	A	n
UGC 5218	12.7 (1.3^2)	195 (4)	182 (4)	3089 (15^3)	A	k
UGC 5326	3.40 (0.3)	118 (7)	92 (4)	1417 (5)	A	a
UGC 5326	4.04 (0.4^2)	124 (4)	101 (4)	1411 (15^3)	A	k
UGC 5326	3.65 (0.4^2)	126 (4)	101 (4)	1413 (4)	A	s
UGC 5358	4.72 (0.5^2)	217 (4)	205 (4)	2914 (15^3)	A	k
UGC 5629	2.89 (0.1)	133 (3)	114 (6)	6203 (5)	A	a
UGC 5651	8.33 (0.8^2)	229 (4)	213 (4)	5568 (15^3)	A	k
UGC 5852	10.9 (1.1^2)	368 (5)	···	6184 (10^3)	G	t
UGC 5852	13.1 (1.3^2)	378 (22^3)	···	6165 (22^3)	A	u
UGC 5852	12.4 (1.2^2)	379 (4)	338 (4)	6177 (4)	A	n
UGC 6018	1.69 (0.2)	72 (3)	51 (3)	1292 (4^3)	A	n
UGC 6018	1.76 (0.4)	65 (7)	48 (5)	1295 (5)	A	a
UGC 6421	7.31 (0.3)	165 (3)	165 (3)	1595 (3)	A	n
UGC 6421	6.59 (0.2)	179 (2)	163 (1)	1504 (4)	A	a
UGC 6464	3.97 (0.4^2)	163 (4)	145 (4)	1071 (15^3)	A	b
UGC 6464	2.60 (0.3^2)	···	125 (8^3)	1067 (8^3)	A	v
UGC 6464	3.11 (0.3^2)	150 (4)	128 (4)	1080 (15^3)	A	k
UGC 6476	3.79 (0.4^2)	300 (4)	322 (4)	7328 (15^3)	A	k
UGC 6872	6.32 (0.6^2)	216 (4)	183 (4)	3205 (15^3)	A	k
UGC 6872	6.52 (0.7^2)	263 (4)	193 (4)	3212 (8)	A	w
UGC 6886	5.54 (0.6^2)	366 (4)	352 (4)	6980 (15^3)	A	k
UGC 6886	5.10 (0.5^2)	394 (4)	360 (4)	6980 (10^3)	A	no
UGC 6886	7.48 (0.7^2)	406 (4)	350 (4)	6972 (8^3)	A	x
UGC 7302	3.87 (0.3)	93 (4)	74 (2)	3838 (4)	A	a
UGC 7302	3.84 (0.4^2)	93 (4^3)	74 (2)	3836 (4)	A	y
UGC 7666	2.54 (0.2)	138 (10)	101 (6)	2559 (5)	A	a
UGC 7976	6.50 (0.7)	98 (4)	75 (4)	2649 (5)	E	z
UGC 7976	5.34 (0.1)	93 (2)	73 (1)	2668 (4)	A	a
UGC 8091	8.70 (0.1)	48 (4)	···	214 (1)	G	l
UGC 8091	7.76 (0.8^2)	41 (4)	27 (4)	213 (15^3)	A	k
UGC 8091	8.60 (1.3)	45 (4)	···	212 (16^3)	B	aa
UGC 8091	5.91 (0.6^2)	46 (4)	30 (4)	214 (···)	A	bb
UGC 8091	6.20 (0.6^2)	40 (4)	26 (4)	214 (10^3)	A	cc
UGC 8091	8.40 (1.1)	38 (4)	24 (4)	214 (22^3)	E	z
UGC 8249	6.95 (0.3)	194 (3)	175 (2)	2541 (4)	A	a
UGC 8249	9.00 (0.4)	195 (4)	···	2545 (···)	G	l
UGC 8503	1.81 (0.2)	71 (6)	40 (4)	4666 (4)	A	a
UGC 8516	4.04 (0.4)	146 (5)	···	1011 (15)	G	t
UGC 8516	4.00 (0.3)	125 (5)	···	1021 (4^3)	A	r
UGC 8516	3.88 (0.4^2)	124 (4)	101 (4)	1025 (15^3)	A	k
UGC 8516	4.19 (0.4^2)	126 (4)	99 (4)	1023 (2)	A	dd
UGC 8896	5.87 (0.6^2)	304 (4)	290 (4)	4401 (15^3)	A	k
UGC 9007	1.42 (0.1^2)	55 (4)	40 (4)	4619 (15^3)	A	k
UGC 9007	1.60 (0.1)	57 (4)	···	4625 (···)	G	l
UGC 9007	1.20 (0.1^2)	148 (4)	62 (11)	4585 (11)	A	ee
UGC 9134	4.65 (1.0)	332 (3)	···	11157 (15^3)	A	ff
UGC 9450	3.05 (1.1)	222 (3)	···	4462 (8)	A	ff
UGC 9450	2.10 (0.2)	213 (12)	180 (7)	4481 (5)	A	a
UGC 9450	3.18 (0.9)	201 (6)	192 (4)	4467 (4)	G	d
UGC 9535	8.61 (0.4)	193 (4)	183 (4)	1792 (15^3)	A	k
UGC 9535	7.99 (2.3)	197 (3)	···	837 (8)	A	ff
UGC 9698	2.86 (1.3)	180 (3)	···	4852 (8)	A	ff

TABLE 3—*Continued*

Name	Flux [Jy km s^{-1}]	W_{20} [km s^{-1}]	W_{50} [km s^{-1}]	v_{HEL} [km s^{-1}]	Tel.[1]	Refs.
UGC 9803	1.69 (1.0)	90 (3)	···	5259 (8)	A	ff
UGC 9803	2.44 (0.6)	82 (17)	45 (11)	5267 (7)	G	d
UGC 9803	1.49 (0.1)	81 (5)	61 (3)	5256 (4)	A	a
UGC 9901	5.79 (2.0)	241 (4)	223 (4)	3161 (15^3)	A	k
UGC 9901	5.27 (0.5^2)	248 (3)	···	3166 (8)	A	ff
UGC 9965	2.40 (0.4)	115 (4)	80 (4)	4525 (8)	A	no
UGC 9965	5.37 (0.5^2)	115 (4)	88 (4)	4528 (15^3)	A	k
UGC 9979	5.44 (0.5^2)	134 (4)	118 (4)	1961 (15^3)	A	k
UGC 9979	5.20 (1.1)	140 (4)	···	1961 (10)	G	l
UGC 10042	4.71 (0.5^2)	349 (4)	337 (4)	4226 (15^3)	A	k
UGC 10243	4.56 (1.9)	161 (3)	···	7937 (8)	A	ff
UGC 10351	5.70 (0.4)	67 (3)	43 (2)	892 (4)	A	a
UGC 10351	9.45 (0.4)	77 (11^3)	48 (2)	891 (4)	G	d
UGC 10384	5.74 (2.3)	382 (3)	···	4970 (8)	A	ff
UGC 10628	6.13 (0.5)	272 (5)	···	2974 (15^3)	G	t
UGC 10628	5.99 (0.6)	259 (4)	240 (4)	2980 (15^3)	A	k
UGC 10628	6.28 (0.2)	259 (6)	244 (5)	6267 (5)	A	b
UGC 10721	6.10 (0.6^2)	286 (4)	267 (4)	2918 (15^3)	A	k
UGC 10747	3.70 (0.4^2)	330 (4)	299 (4)	8820 (15^3)	A	k
UGC 10901	8.33 (0.3)	198 (3)	178 (2)	2834 (4)	A	a
UGC 11017	3.74 (0.3)	189 (6)	167 (4)	4648 (4)	A	a
UGC 11017	1.40 (0.4)	149 (4)	143 (4)	4628 (13)	A	no
UGC 11120	3.58 (0.2)	179 (3)	162 (2)	2242 (4)	A	a
UGC 11285	5.01 (0.2)	321 (5)	299 (3)	4500 (4)	A	a
UGC 11362	3.74 (0.2)	207 (4)	190 (3)	4204 (4)	A	a
UGC 11461	8.10 (0.9)	302 (12)	286 (8)	3121 (4)	N	h
UGC 11482	8.21 (0.3)	289 (2)	273 (1)	3163 (4)	A	a
UGC 11482	9.04 (1.5)	271 (6)	287 (10)	3157 (5)	G	d
UGC 11504	3.50 (0.4)	168 (12)	128 (19)	5619 (7)	A	a
UGC 11578	8.69 (0.3)	96 (2)	73 (2)	4604 (4)	A	a
UGC 11578	11.8 (0.7)	103 (5)	77 (3)	4602 (4)	G	d
UGC 11624	2.91 (0.2)	218 (4)	201 (3)	4831 (4)	A	a
UGC 11627	2.14 (0.2)	135 (9)	114 (6)	4864 (5)	A	a
UGC 11627	1.18 (0.4)	117 (19)	195 (7)	4866 (5)	G	d
UGC 11655	3.81 (0.6)	273 (17)	247 (11)	4761 (7)	G	d
UGC 11655	3.26 (0.8)	277 (9)	255 (6)	4756 (5)	A	a
UGC 11655	4.19 (0.7)	269 (3)	259 (3)	4756 (3)	A	gg
UGC 11708	8.39 (0.8^2)	302 (4)	283 (4)	4161 (4)	A	k
UGC 11774	3.48 (0.3)	255 (9)	228 (6)	6878 (5)	A	a
UGC 11774	3.92 (0.4^2)	245 (8^3)	228 (8^3)	7126 (8^3)	A	e
UGC 11849	5.09 (0.8)	361 (3)	339 (3)	5841 (1)	A	gg
UGC 11849	3.60 (0.8)	337 (25)	320 (17)	5834 (8)	N	h
UGC 11926	5.29 (0.5^2)	111 (8^3)	99 (8^3)	1649 (8^3)	A	e
UGC 11926	6.19 (0.3)	115 (3)	97 (2)	1651 (4)	A	a
UGC 11992	5.43 (0.3)	184 (3)	167 (2)	3596 (4)	A	a
UGC 11992	7.12 (1.1)	181 (11)	162 (7)	3596 (5)	G	d
UGC 12094	2.27 (0.2)	73 (6)	41 (4)	7614 (4)	A	a
UGC 12094	1.14 (0.2)	62 (3)	32 (3)	7604 (3)	A	gg
UGC 12158	4.87 (0.5^2)	178 (8^3)	156 (8^3)	9290 (8^3)	A	e
UGC 12388	5.42 (0.2)	281 (4)	261 (3)	4585 (4)	A	a
UGC 12537	3.81 (0.6)	466 (3)	441 (3)	6116 (2)	A	f
UGC 12624	3.05 (0.3^2)	184 (8^3)	164 (8^3)	3519 (8^3)	A	e
UGC 12624	3.19 (0.3)	211 (11)	183 (7)	3517 (5)	A	a
UGC 12695	6.06 (0.6)	87 (6)	64 (4)	6184 (4)	A	a
UGC 12695	2.80 (0.8)	79 (18)	63 (12)	6189 (6)	N	h
UGC 12695	5.16 (0.5^2)	92 (4)	67 (4)	6184 (4)	A	o
UGC 12910	3.36 (0.3)	86 (7)	53 (4)	6352 (4)	A	a
CAP 0718+06	1.50 (0.1)	···	199 (4)	1141 (4)	A	hh
Malin 1	3.50 (0.5)	341 (4)	···	24750 (9^3)	A	ii
Malin 1	4.60 (0.5^2)	340 (4)	315 (4)	24745 (10^3)	B	jj
Malin 1	2.70 (0.3^2)	355 (4)	295 (4)	24705 (10^3)	A	jj
[OBC97] P02-3	1.82 (0.2)	112 (5)	95 (5)	3178 (5)	A	kk

TABLE 3—*Continued*

Name	Flux [Jy km s^{-1}]	W_{20} [km s^{-1}]	W_{50} [km s^{-1}]	v_{HEL} [km s^{-1}]	Tel.[1]	Refs.
[OBC97] P07-1	1.43 (0.1)	187 (5)	177 (5)	7949 (5)	A	kk
[OBC97] U01-4	1.93 (0.2)	191 (5)	181 (5)	3450 (5)	A	kk

NOTE.—[1] Telescopes: A= Arecibo 305m telescope; G = Green Bank 300ft telescope; N = Nancay Decimetric Radio Telescope; W = Westerbork Synthesis Radio Telescope; J = Jodrell Bank 250ft Telescope; E = Effelsberg 100m telescope; B = Green Bank 140ft Telescope.
[2] Not given in the literature, and estimated from assuming a 10% flux error.
[3] Not given in the literature, and estimated from 0.5*channel resolution.

References. — a. Schneider, Thuan, Magri, & Wadiak (1990); b. Giovanardi & Salpeter (1985); c. Bothun et al. (1984); d. Schneider, Thuan, Mangum, & Miller (1992); e. Giovanelli & Haynes (1993); f. Giovanelli & Haynes (1985); g. Haynes et al. (1997); h. Theureau et al. (1998); i. Roelfsema & Allen (1985); j. Staveley-Smith & Davies (1987); k. Lewis, Helou, & Salpeter (1985); l. Tifft & Cocke (1988); m. Giovanelli & Haynes (1989); n. Bicay & Giovanelli (1986); o. Lewis (1987); p. Bicay & Giovanelli (1986); q. Giovanelli & Haynes (1985); r. Haynes & Giovanelli (1984); s. Schneider, Helou, Salpeter, & Terzian (1986); t. Peterson (1979); u. Davis & Seaquist (1983); v. Helou, Salpeter, & Terzian (1982); w. Huchtmeier & Richter (1989); x. Hoffman et al. (1989); y. Fontanelli (1984); z. Huchtmeier & Richter (1987); aa. Hunter & Gallagher (1985); bb. Hoffman, Helou, Salpeter, & Sandage (1985); cc. Lewis (1984); dd. Oosterloo & Shostak (1993); ee. Bothun et al. (1985a); ff. Freudling, Haynes, & Giovanelli (1988); gg. Giovanelli, Myers, Roth, & Haynes (1986); hh. Pantoja, Altschuler, Giovanardi, & Giovanelli (1997); ii. Bothun, etal. (1986); jj. Impey & Bothun (1989); kk. O'Neil, Bothun, & Schombert (2000); ll. Richter & Huchtmeier (1991).